



# Quaternary coral reef complexes as powerful markers of long-term subsidence related to deep processes at subduction zones: Insights from Les Saintes (Guadeloupe, French West Indies)

Frédérique Leclerc<sup>\*†</sup> and Nathalie Feuillet<sup>\*</sup>

Institut de Physique du Globe de Paris, Université Sorbonne Paris Cité, Paris Diderot Université UMR 7154, Centre National de la Recherche Scientifique, F-75005 Paris, France

## ■ ABSTRACT

**Geodetic measurements reveal modern rates of tectonic deformation along subduction zones, but the kinematics of long-term deformation are typically poorly constrained. We explore the use of submarine coral reefs as a record of long-term coastal vertical motion in order to determine deformation rate and discuss its origins. The Lesser Antilles arc results from the subduction of the American plates beneath the Caribbean plate and undergoes regional vertical deformation. Uplifted reefs along forearc islands are markers of the interplay between tectonics and sea-level variations since the late Pleistocene. We compared results from a numerical model of reef-island profile development to high-resolution marine geophysical measurements of Les Saintes reef plateau (Guadeloupe, French West Indies), a ~20-km-wide, 250-m-thick submerged platform that lies at 45 m below sea level along the volcanic arc, to constrain its vertical deformation history. Models explore different scenarios over wide parameter domains including start time, basement morphology, sea level variations, reef growth rate, subaerial erosion rate, and vertical motion history. The major features of the plateau (its depth, internal structure, unusual double-barrier) is only reproduced in a context of subsidence, with a constant rate of  $-0.3$  to  $-0.45$  mm/yr since the late Pleistocene, or in a context of increasing subsidence, presently of  $\sim -0.2$  mm/yr. Discussed in the framework of the forearc vertical deformation history, this result indicates subsidence is promoted by local faulting, volcanic, and deep subduction processes. Coseismic deformation accumulation could be a mechanism by which deformation builds up in the long-term. We show that subduction can drive long-term subsidence of a volcanic arc, and demonstrate that submarine reefs are powerful markers of long-term vertical motion.**

## ■ INTRODUCTION

Subduction megathrusts are generally expected to behave elastically over time intervals of years to decades (Savage, 1983). Measurements of surface

\*E-mail: [leclerc@geoazur.unice.fr](mailto:leclerc@geoazur.unice.fr); [feuillet@ipgp.fr](mailto:feuillet@ipgp.fr)

<sup>†</sup>Now at Géoazur, Université Nice Sophia Antipolis (Université Côte d'Azur, Centre National de la Recherche Scientifique, Institut de Recherche pour le Développement, Observatoire de la Côte d'Azur), Géoazur UMR 7329, 250 rue Albert Einstein, Sophia Antipolis 06560 Valbonne, France

deformation above subduction megathrusts using GPS, InSAR (e.g., Chlieh et al., 2004), and coral microatolls (e.g., Zachariasen et al., 2000) are generally consistent with this idea. Along the Sumatra-Andaman megathrust, Indian Ocean, co-, inter-, and post-seismic vertical deformations (called short-term deformation in the following) seem to compensate each other over a few seismic supercycles (Sieh et al., 2008; Philipposian et al., 2017).

But this is not always verified. Instead, the coasts of most active converging margins appear to be uplifting (see the review in Pedoja et al., 2014) over several hundreds of thousands of years and more (a time scale termed “long-term” in the following), and many authors are now considering the possibility that megathrust seismic activity can drive short-term deformation that is able to accumulate in the upper-plate (e.g., Taylor et al., 1980; Wesson et al., 2015, and Baker et al., 2013). Other processes that contribute to long-term deformation, which may include subducting seamounts (e.g., Taylor et al., 2005; De Min et al., 2015; Saillard et al., 2011), accretion or erosion processes at the plate interface (e.g., Vannucchi et al., 2013), and upper-plate structures as splay faulting (e.g., Melnick et al., 2012; Wang et al., 2013; Jara-Muñoz et al., 2017), likely influence megathrust mechanical behavior and seismic cycles (Béjar-Pizarro et al., 2013), yet these processes remain poorly understood. One way to improve this situation is to determine the extent, direction, and amplitude of past tectonic movements along subduction zones.

Along active margins, surface features such as alluvial, marine, or reef terraces are especially valuable as vertical deformation markers (e.g., Saillard et al., 2011; Jara-Muñoz et al., 2015). In tropical areas, Quaternary reef deposits that initially formed offshore can be outcropping on land at several tens to hundreds of meters above sea level (masl), where they form flights of reef terraces along the island coasts. They can be dated and their altitude measured in order to estimate the vertical deformation of the coasts. Along most active margins, such markers are usually rare or they are distributed unevenly. Most of the time, they are only studied on land as they can be identified more easily than offshore (see the worldwide database of such markers in Pedoja et al., 2011), biasing the picture of the deformation along active margins for instance (e.g., Henry et al., 2014).

In this paper, we show that tectonic displacement of shallow-water submarine reefs can provide insight into the long-term vertical motion history of subduction zones. We propose a combined methodology to constrain past

tectonic movements using submarine coral reef morphology and stratigraphy associated with reef growth modeling, applied to Les Saintes volcanic islands, Guadeloupe, French West Indies, in the Lesser Antilles arc.

In the Lesser Antilles, the Caribbean and American plates converge at a rate of only 2 cm/yr (Fig. 1; DeMets et al., 2000). In the Guadeloupe forearc, along the coasts of Marie-Galante, La Désirade, and Grande-Terre islands, quaternary reef deposits are outcropping on land at several tens of masl (Tables 1 and 2). They form flights of reef terraces along the island coasts, surrounding high plateaus formed of Plio–Pleistocene carbonate platform deposits (Andreieff et al., 1989; Cornée et al., 2012; Münch et al., 2014). These geologic evidences indicate the forearc has experienced long-term vertical deformation, during the Plio–Quaternary (e.g., Feuillet et al., 2004; Münch et al., 2014), likely linked to subduction processes (Feuillet et al., 2004; De Min et al., 2015). But the picture of the deformation is incomplete here, in particular along the volcanic arc, to discuss the processes at work. Recent studies have shown that in the Lesser Antilles, the down-dip limit of the seismogenic zone is much deeper and therefore much closer to the volcanic islands than previously thought (Laigle et al., 2013; Weil-Accardo et al., 2016; Paulatto et al., 2017). Therefore, upper-plate deformation could extend farther in the upper-plate, toward the volcanic arc, and needs to be investigated.

Along the coasts of the volcanic islands (Les Saintes and Basse-Terre), no Quaternary reef deposits are found onland (e.g., Vérati et al., 2016; Battistini et al., 1986). Offshore, large, submerged reef complexes have developed over the Quaternary (Fig. 1; Macintyre, 1972), along the forearc islands but also along the volcanic arc, and as their counterparts on land, equally retain a record of the islands' tectonic movements. Les Saintes archipelago particularly exhibits a valuable vertical deformation marker in this tropical area: a drowned reef platform.

Using high-resolution bathymetric data and seismic profiles, we first characterize the morphology and stratigraphy of Les Saintes carbonate platform, 280 km away from the trench, where, until now, there have been no estimates of vertical motions. We explore the ways a carbonate platform can gain such morphology and stratigraphy, by investigating in particular the impact of the vertical movements of the coasts. Through extensive reef growth modeling, we explored different scenarios testing the variability of different parameters on the modeled morphology and stratigraphy. These parameters include the start time, the basement morphology (slope and presence of fault scarp) and the sea level variations and their uncertainties that are still debated (e.g., Siddall et al., 2007). We also tested over wide ranges, different reef growth rate, subaerial erosion rate, and vertical motion history. We show that the platform acquired its shape and structure in a context of subsidence, and we investigate if and how the subsidence might have changed through time.

This result allows us to complete the pattern of long-term deformation of the Guadeloupe archipelago over the past few hundreds of thousands of years from the forearc to the volcanic arc. We then consider the different mechanisms that could have driven this accumulated deformation over time in Les Saintes, and in the Lesser Antilles arc.

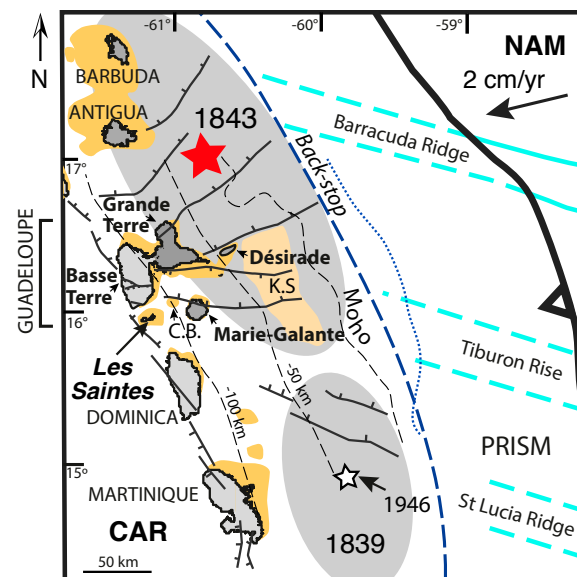


**Figure 1.** Tectonic context of the Guadeloupe archipelago and Les Saintes islands, French West Indies. North American (NAM) and South American (not shown) plates converge toward the Caribbean (CAR) plate at 2 cm/yr (DeMets et al., 2000), generating the Lesser Antilles arc. The forearc islands, capped by Plio–Pleistocene carbonate platforms are mapped in dark gray whereas volcanic islands are in light gray. Submarine coral reef platforms are in orange, with Colombie Bank (C.B.) and Karukera Spur (K.S.). Blue lines show back-stop locations estimated from gravity (thick dashed blue line; Bowin, 1976) and seismic studies (dotted thin blue line; Paulatto et al., 2017). Dashed black thin lines are iso-depths of the plate interface and its contact with the over-riding plate's Moho (Paulatto et al., 2017). The red star shows the epicenter of the Mw>8 1843 earthquake that probably ruptured the plate interface, while gray areas represents the probable rupture extent of the 1843 and 1839 earthquakes (Feuillet et al., 2011a). The white star shows the epicenter of the 21 May 1946 earthquake in front of Martinique (Feuillet et al., 2011a). The active margin is bordered by the up-to 300-km-wide Barbados accretionary prism that is deformed by three subducting ridges Barracuda Ridge, Tiburon Rise, and St. Lucia Ridge (Laigle et al., 2013 and references therein), represented in cyan. Locations of normal faults that accommodate slip partitioning along the plate boundary are indicated (thin black lines, Feuillet et al., 2010).

## ■ MORPHOLOGY AND SEISMIC STRATIGRAPHY OF LES SAINTES SUBMARINE PLATEAU

Les Saintes archipelago lies between Basse-Terre and Dominica, along the volcanic arc that built since the late Miocene (Jacques and Maury, 1988). Along the coasts of the volcanic islands (Les Saintes and Basse-Terre), no Quaternary reef deposits are found onland (e.g., Vérati et al., 2016 for a recent geological map of Les Saintes, see also Battistini et al., 1986 for a review), except a few

TABLE 1. DISTRIBUTION AND ALTITUDE OF MIS5 REEF TERRACES IN THE GUADELOUPE ARCHIPELAGO, FRENCH WEST INDIES

Islands	Altitude of the terrace inner-edges (m)	Data type; References
<u>La Désirade</u>		
East	10	Dates; Lardeaux et al. (2013)
West	10	Dates; Lardeaux et al. (2013), Léticée et al. (2019), Battistini et al. (1986), Feuillet et al. (2004)
<u>Marie-Galante</u>		
East	10	Dates; Battistini et al. (1986), Feuillet et al. (2004)
West	2–3	Inferred; Battistini et al. (1986), Feuillet et al. (2004), Bouysse et al. (1993)
<u>Grande-Terre</u>		
East (Gros Cap)	5–6	Dates; Battistini et al. (1986)
North (Anse Laborde)	3–5	Dates; Battistini et al. (1986)
Northwest (Anse Gris-Gris)	(30 cm*)	Dates; Weil-Accardo (2014)
Southwest	Not reported on land	Battistini et al. (1986)
Basse-Terre	Not reported on land	Battistini et al. (1986)
Les Saintes	Not reported on land	Battistini et al. (1986)

\*The MIS5e terrace does not form a morphologic terrace along the western coast of Grande-Terre, no shoreline angle was measured. The MIS5e deposit was found below the mangrove, and a sample recovered at 30 cm was dated.

small deposits that were dragged up by explosive volcanic activity in Basse-Terre, and are therefore non-relevant to this study. Offshore, Les Saintes reef plateau formed on the remnant of volcanic edifices.

High-resolution bathymetry with a resolution of 10 m/pixel (BATHYSAINTES cruise, Deplus and Feuillet, 2010; see Leclerc et al., 2014, for extensive description) and 6-channel seismic reflection profiles from sparker sources (KaShallow cruises, Lebrun, 2009; see Münch et al., 2013 for details on data processing) were acquired on the drowned reef plateau around the Saintes Islands (Fig. 1) allowing morphological and structural studies of the platform.

The bathymetric data show that the reef platform surrounding the Saintes Islands is up to 23 km wide (Figs. 2A, 2B) and has a minimum vertical relief of 250 m (from sea level to the slope break at the base of its cliff, Fig. 2B). The morphology of the reef platform is extensively described in Leclerc et al. (2014) and therefore only summarized in the following. Close to the islands, a small, shallow terrace lies at a mean depth of 25 m below sea level (mbsl), Figs. 2A and 2C). Seaward, the platform forms a plateau that is overall flat and lies between 38 and 60 mbsl, with an average depth of  $\sim 45 \pm 5$  mbsl (Fig. 2). Small NW-SE-striking normal faults crosscut and offset its surface by up to

TABLE 2. DISTRIBUTION AND ALTITUDE OF (A) THE UPPER PLATEAU OF THE GUADELOUPEAN FOREARC ISLANDS, FRENCH WEST INDIES AND (B) OF THE REEF DEPOSITS OF PROBABLE MIS7 AGE

Islands	(A) Altitude of the upper plateau (masl)**	(B) Altitude of the MIS7 deposits
<u>La Désirade</u>		
Summit	276 m	-
<u>Marie-Galante</u>		
East	150 m	~75 m*
Southwest	100 m	~50 m*
<u>Grande-Terre</u>		
Northern Plateau		
Northeast (south of Gros Cap)	70 m	-
Northwest (Port-Louis)	10 m	-
Eastern Plateau	-	(25 m)#
<u>Basse-Terre</u>		
Versaille Borehole##	-79 m	

\*Villemant and Feuillet (2003) dated several samples from terrace T2, and applied an open-system model that gives an age of  $249 \pm 8$  ka for this terrace (MIS7.5).  
 \*\*Altitude of the upper plateaus, measured far from faults, or corrected from fault induced offset and elastic flexure when possible (Feuillet et al., 2004).  
 #Villemant and Feuillet (2003) dated one sample at Pointe des Chateaux, found at 25 m, by U-Th method. This altitude is not a shoreline angle, that must be equal or higher. Without age-model correction, it gives an age of  $277 \pm 11$  ka. Feuillet et al. (2004) propose that it formed at the same time as T2, the sample age being older as not corrected with an open-system model.  
 ##Garrabé and Paulin, 1984.  
 masl—meters above sea level.

8 m. They belong to the regional fault system that crosscuts Les Saintes area (Feuillet et al., 2011b; Leclerc et al., 2016).

The plateau displays surface features typical of a reef carbonate platform (Fig. 2A; Leclerc et al., 2014): pinnacles; a barrier reef on the plateau's edge, including an unusual double barrier to the NE bounding a 0.5–1-km-wide depression. The inner and outer barriers are on average a few meter high above the plateau floor, except where pinnacles developed. This type of double-barrier forms in particular conditions either where strong currents affect the coral reef (Coudray, 1976) or when reef growth migrates through time from the inner to the outer reef, due to eustatism or tectonics (Andréfouët et al., 2009). Spurs and grooves built behind the double-barrier in the direction of southwestward flowing currents are also present. These features have morphology similar to the ones of modern reefs, and do not show evidence of subaerial erosion. They were built during sea level rise following the Last Glacial Maximum (LGM). They are however presently drowned at  $\sim 45$  mbsl.

Several seismic profiles were acquired and image the carbonate platform (Figs. 3 and 4). The profiles reveal a stratigraphy composed of seismic units that are stacked vertically and separated by erosion surfaces that naturally dip

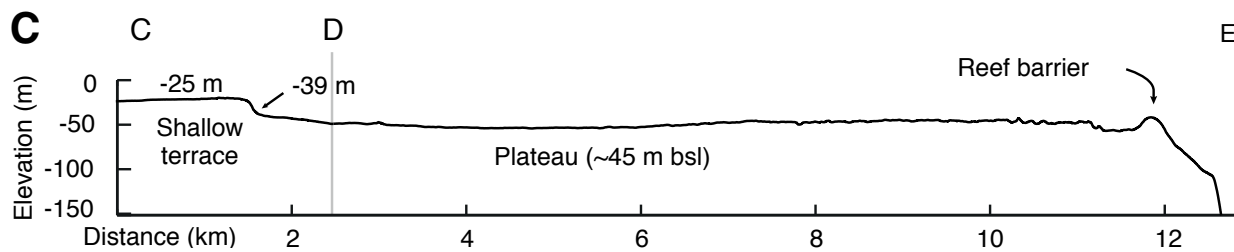
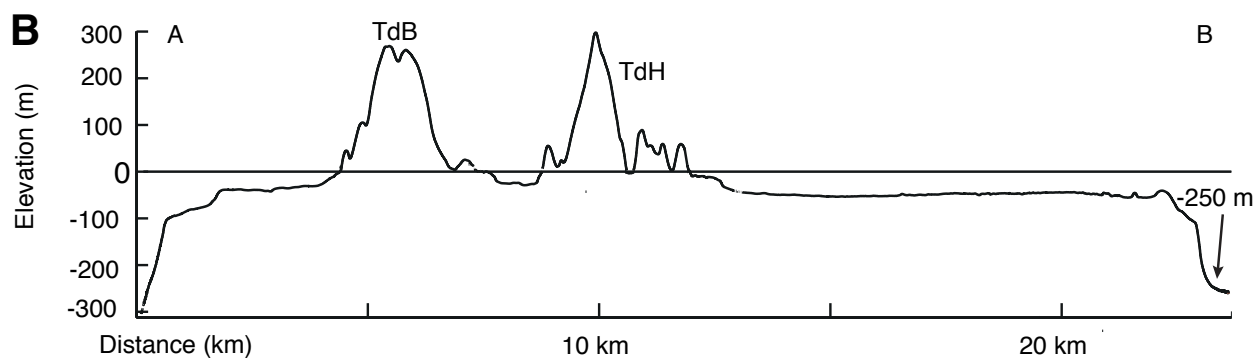
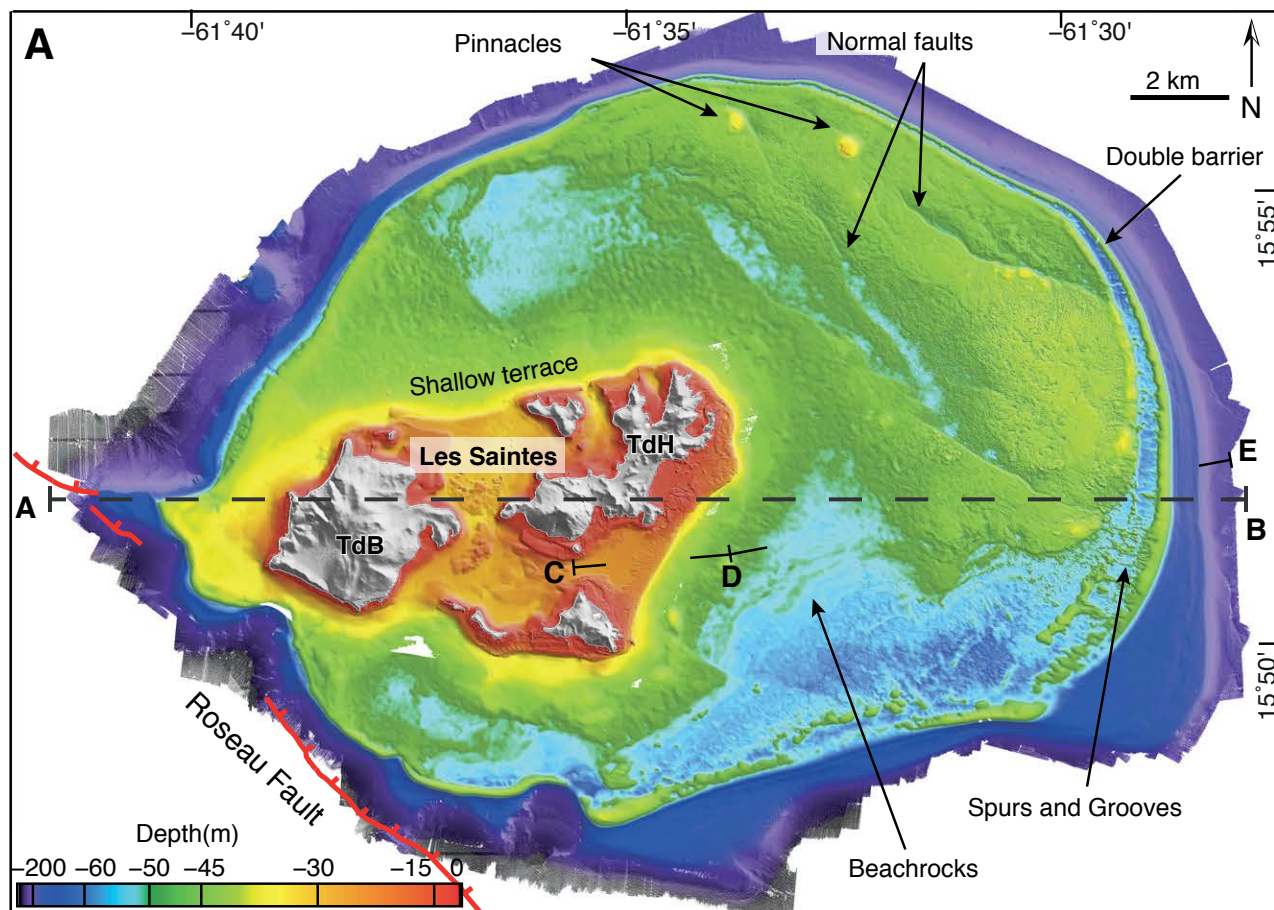
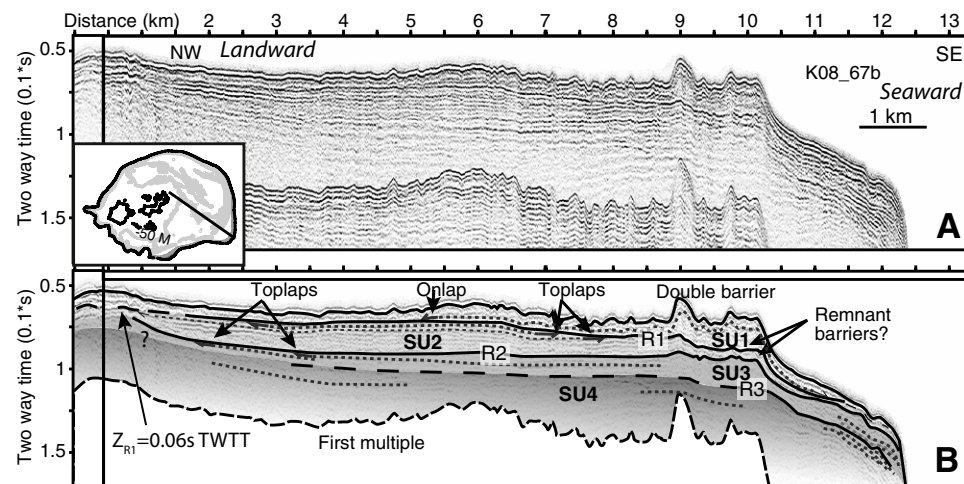


Figure 2. Morphology of Les Saintes plateau, Guadeloupe, French West Indies. (A) Bathymetry and (B, C) bathymetric profiles of the reef platform of Les Saintes archipelago, AB and CDE located on (A). The platform displays a fringing reef (in red shades in 2A, with depth >15 mbsl), a shallow terrace at ~25 mbsl (in orange to yellow shades in 2A), and a wide plateau drowned at ~45 mbsl (see text for description, and Leclerc et al., 2014). Vertical gray line in (C) marks the kink in the transect CDE located on the map. TdB – Terre de Bas Island; TdH – Terre de Haut Island.



**Figure 3.** (A) Seismic data and (B) interpretation of the 6-channel seismic profile K08\_67b, modified from Leclerc et al. (2014). Inset shows the location of the profile on Les Saintes plateau, Guadeloupe, French West Indies. High-amplitude reflectors marked R1, R2, and R3, separate the four seismic units SU1, SU2, SU3, and SU4, colored in light to dark gray. Inner reflectors (dashed gray lines ended by arrows) top lap or onlap the surfaces R1, R2, and R3. TWTT—two-way travel time.

seaward (Figs. 3 and 4). This structure is typical of reef platforms that have accreted as accommodation space is created by subsidence and/or erosion (Rooney et al., 2008). This is particularly visible on the profile K08\_71b that is perpendicular to the fault system (Figs. 4A, 4B), but also on the two radial profiles K08\_67 and K08\_69 (Figs. 3, 4C, and 4D). Under the uppermost Seismic Unit 1 (SU1) that is composed of the reef features evidenced in the bathymetry, we identify three other sedimentary packages (SU2, SU3, and SU4) whose tops and bottoms are marked by strong reflectors ( $R_1$ ,  $R_2$ , and  $R_3$ ; Figs. 3, 4C, and 4D). The inner reflectors of SU2 top lap  $R_1$ , whereas those of SU1 onlap  $R_1$  (Fig. 3). Similarly, the inner reflectors of SU3 top lap  $R_2$ , whereas those of SU2 onlap  $R_2$  (Figs. 3, 4D, and 4C). This architecture indicates periods of sea level drop and erosion (forming  $R_1$  and  $R_2$ ), followed by transgressions (Fig. 3). The geometric relation of reflector  $R_3$  and inner reflectors of SU3 and SU4 are less clear in the seismic profiles. All reflectors  $R_1$ ,  $R_2$ , and  $R_3$  are dipping seaward, and are close to merge landward (Fig. 3). The seismic stratigraphy provides evidence for single or double barrier reef morphology along the plateau's edge above  $R_3$ , suggesting that SU2 and SU3 are also constituted by reef units built on the plateau's edge. Landward, these seismic units present parallel reflectors that can be associated to back-reef and lagoonal sedimentation.

To quantify seismic units' depth and thickness, seismic travel times were converted to depth assuming a wave velocity of 1500 m/s through the water column. In carbonates, seismic wave velocities have shown to be scattered between 1500 and 6500 m/s (Anselmetti and Eberli, 2001; Camoin et al., 2007), and do not increase systematically with depth (Anselmetti and Eberli, 1993), the last-deglacial carbonate sequence showing smaller  $V_p$  than the older Pleistocene sequence (Camoin et al., 2007). Taking into account this scattering and its nature, and the fact that in the following we only determine shallow features' depth and thickness, systematically away from fore-reef structures (that present

higher velocities), but in back-reef environments, we chose to calculate the depth of seismic reflectors by using low seismic velocities, ranging between 1500 and 3000 m/s in the platform.

Along the seismic profiles, close to the island coast and under the back-reef area of SU1, the shallowest reflector lies at a depth  $Z_{R1}$  of 0.06 s two-way travel time (TWTT) (Fig. 3), composed of 0.05 s TWTT in water and 0.01 s TWTT in carbonates.

By using a velocity of 1500 m/s in water and a velocity ranging from 1500 to 3000 m/s in carbonates, the reflector  $R_1$  reaches a minimum depth  $Z_{R1}$  of  $49 \pm 4$  mbsl.

Along the seismic profile K08\_67b (Fig. 3), we can notice the three reflectors  $R_1$ ,  $R_2$ , and  $R_3$  deepen seaward. Within the domain bracketed by the cliff of the 25 mbsl terrace, and the reef barrier, we estimated the depths of the three reflectors  $R_1$ ,  $R_2$ , and  $R_3$  at three locations along the profiles: kilometer 2, 5, and 8. Reflector  $R_1$  deepens from 0.069 s TWTT landward (at kilometer 2), to 0.08 s TWTT (at kilometer 8) and reflector  $R_2$  deepens from 0.069 to 0.093 s TWTT (at kilometer 2 and 8, respectively). Reflector  $R_3$  is less easy to follow, but it seems to deepen too, from 0.101 to 0.105 s TWTT (at kilometer 5 and 8, respectively).

By using the velocity values discussed above, we can estimate that the three reflectors  $R_1$ ,  $R_2$ , and  $R_3$  lie between 52 and 71 mbsl, 63–90 mbsl, and 76–109 mbsl, respectively.

## REEF GROWTH MODEL METHODOLOGY

To determine the conditions of vertical coastal movement compatible with these morphologic and stratigraphic observations, we turn to a numerical model of reef growth.

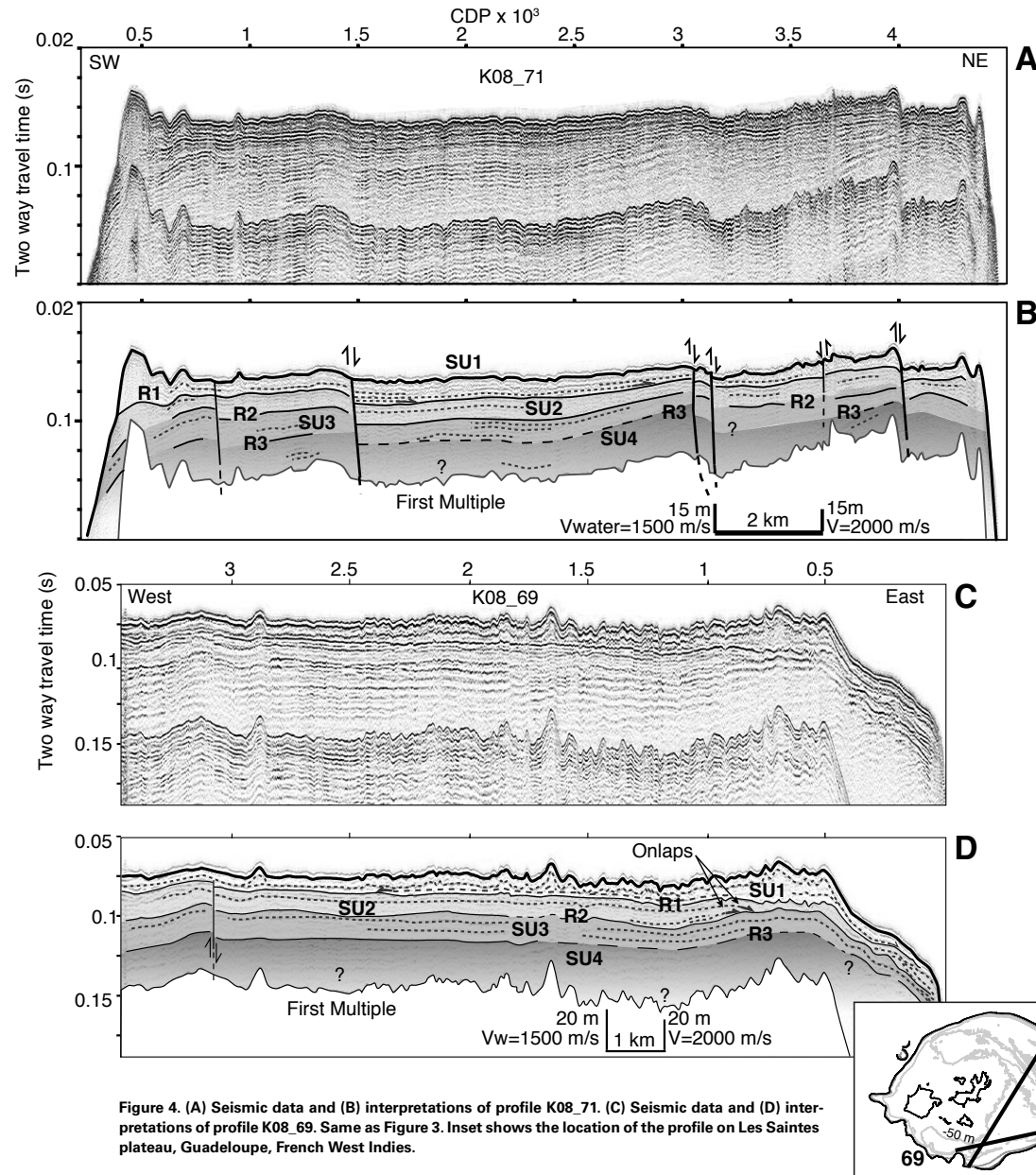


Figure 4. (A) Seismic data and (B) interpretations of profile K08\_71. (C) Seismic data and (D) interpretations of profile K08\_69. Same as Figure 3. Inset shows the location of the profile on Les Saintes plateau, Guadeloupe, French West Indies.

### Description of the Model

Numerical experiments used a simple 2-D reef-profile model, adapted from Toomey et al. (2013) where the model is described in detail. The model domain consists of an initial linear island slope (Fig. 5) that is then shaped by reef growth (G), island vertical motion (U), wave erosion and sediment transport, subaerial erosion (E). Changes in sea level occur at 50 year intervals and the model simulation spans a certain period of time starting from an initial time ( $T_0$ ). Vertical motion rate ( $U > 0$  for uplift,  $U < 0$  for subsidence) is fixed across the entire model domain, while subaerial erosion ( $E > 0$ ) is applied to parts of the model that are standing above the sea. Vertical reef accretion (G) is simulated using Bosscher and Schlager's (1992) parameterization of coral growth as a declining function of water depth and light attenuation, as described in Toomey et al. (2013). Reef accretion and wave erosion only occur between the reef's seaward edge and a point 200 m landward of the reef crest, with wave erosion occurring only when the reef surface is within 2 m of the sea surface. Sediment generated by wave erosion of the reef is deposited either within the lagoon if one exists, or offshore, on the reef front, at the angle of repose. Primary production of carbonate sediment in the water column also occurs in the lagoon at a fixed rate (0.2 m/k.y., Zinke et al., 2001).

On the basis of the morphological analyses and seismic reflection data of Les Saintes plateau, we consider a model good, and therefore a parameter combination satisfying, when the model generates a set of constraints: a fringing reef, a plateau drowned at  $45 \pm 5$  mbsl, and an internal structure composed of vertically stacked units, with the shallower surface of erosion reaching a depth landward of  $49 \pm 4$  mbsl (equivalent to the depth of  $Z_{R1}$  close to the coast, and named in the models  $Z_{E1}$ , Fig. 5).

### Free Variables for Les Saintes Simulations

Little is known about the values of certain parameters to be applied in order to reproduce Les Saintes plateau morphology, and to constrain the vertical motion rate that is our main unknown parameter. To counterbalance this, we carried out sensitivity tests on these free variables: age and bathymetry of the initial condition ( $T_0$  and slope), sea level history, maximum reef growth rate, subaerial erosion rate, all of them are described below (see also Table 3 that sums up variables names). We changed the value of one parameter at a time, over a wide range, and explored the model results in order to reproduce Les Saintes plateau morphology and to estimate vertical motion rate with the least prejudice.

#### Start Time $T_0$

Les Saintes reef plateau formed on the remnant of volcanic edifices that are several Ma old. The youngest volcanic edifices are dated at 600 ka (Jacques and

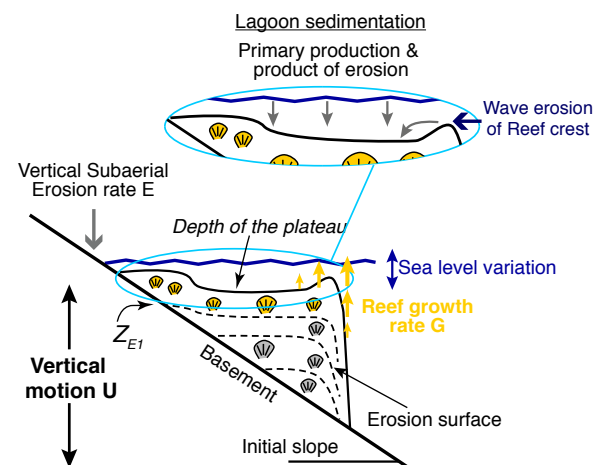


Figure 5. Conceptual sketch of the reef growth model we used to reproduce the morphology of Les Saintes plateau, Guadeloupe, French West Indies. See main text and Toomey et al. (2013) for full description of the model.

Maury, 1988), revised recently at 800 ka (Zami et al., 2014). Reef construction might have started along the submarine volcanic slopes at shallow depth as soon as substrates were adequate for coral growth, but we lack constraints on this start time in Les Saintes, such as dates or seismic stratigraphy of the plateau deeper than 100 mbsl.

In the Lesser Antilles, Adey et al. (1977) noticed that reefs are poorly developed along the slopes of active volcanoes (also evidenced in Martinique on the basis of shallow bathymetric data; Leclerc et al., 2015). Volcanic activity induces acidic and turbid waters as well as poorly consolidated slopes that do not favor reef growth (Adey and Burke, 1976; Adey et al., 1977). Therefore, a time delay can exist between the arrest of the volcanic activity and the settlement of reefs.

TABLE 3. LIST AND VALUES OF PARAMETERS USED IN THE REEF GROWTH MODEL

Name	Significance and units	Tested values
G	Reef growth rate (m/k.y.)	0.5 to 10, every 0.5
U	Vertical motion (m/k.y.)	0 to -0.8, every 0.05
E	Subaerial erosion rate (m/k.y.)	0 to 0.15, every 0.05
$T_0$	Start time of the model (ka)	600–400–330
$Z_{R1}$	Depth of the shallowest reflector interpreted as a surface of erosion	45 to 71 mbsl
$Z_{E1}$	Depth of the shallowest modeled surface of erosion, at its intersection with basement	See Figure 7

Note: mbsl—meters below sea level

Thus, we focused our models on reasonable start times that postdate the end of volcanic activity. We set  $T_0$  at 600 ka, 400 ka, and 330 ka. Our choice is also motivated by the fact that if we assume a constant vertical motion story, the older the start time  $T_0$  the thicker the modeled plateau, exceeding 250 m in thickness. In the following, we test different  $T_0$  in order to quantify and discuss the sensitivity to this parameter on the vertical motion rates needed to reproduce Les Saintes plateau morphology and stratigraphy.

### Initial Bathymetry: Slope and Fault

It has been shown that basement morphology can influence the morphology of the carbonate platform, offering a wider or thinner surface on which the reef can develop (Cabiocch, 2003). We therefore tested the influence of the initial basement shape on reef construction. The islands in the Saintes archipelago are the remnants of ancient volcanoes. We consequently hypothesized the shape of the volcanic construction prior to platform growth to be conical (or linear along a transect) like modern subaerial or submarine active volcanoes (see for example the nearby submarine Colibri volcano, in the Les Saintes channel in Leclerc et al. (2016)). A batch of models was run with this linear slope, for two initial slope values, 0.075 m/m and 0.02 m/m, which would correspond, respectively, to the western and eastern slope of the islands, calculated between the coast and the slope break at ~250 mbsl. We also ran models that take into account the fact that the modern Les Saintes plateau is offset by small normal faults. These faults have 5–8-m-high scarps on the plateau, whereas they can have scarps up to 50 m high southward, in the Saintes Trough (Leclerc et al., 2016, see Marigot and Pompierre faults). This system initiated after the main volcanic construction in the area, and faulting has certainly offset the volcanic slopes of the Les Saintes volcanic edifice prior to reef settlement. To understand how faulting has influenced platform development and morphology, we ran a model for an initial slope of 0.02 that is offset in its middle by a 20-m-high scarp, and in another batch by a 40-m-high scarp. Slip rate on these faults is probably only a few tenths of a meter per k.y. (or tenths of mm/yr, Leclerc et al., 2016). Consequently, we did not model the fault activity during the reef accretion, as fault slip rate is one order of magnitude slower than the reef accretion rate (discussed below).

### Sea-Level History

Over the past few hundreds of thousands of years, the sea level has varied in relation with climate, being low during glacial periods (~120 mbsl, during LGM, ~20 k.y. ago), and high during interglacial periods as today. For the last 500 k.y., independent proxies have allowed to document the sea level variations through time (e.g., Rohling et al., 2014). But due to the proxies' nature and sampling locations, large variations for a single sea level highstand exist

in the different data sets (e.g., Siddall et al., 2007), uncertainties increasing with age. During the last interglacial period (ca. 125 ka), called MIS5e, the sea level was higher than today, and several authors estimate it peaked at ~5–6 masl, and might have exceeded 8 m (Kopp et al., 2009) or even 9 masl (Dutton and Lambeck, 2012). Siddall et al. (2007) reviewed the constraints on the sea level for the last interglacials. The sea level during MIS7a (193–201 ka), and also during MIS7c and MIS7e, probably reached an altitude between –5 and –15 m. During MIS9c, the sea level highstand occurred 331 ka, and might have reached –3 to +8 m (Schellman and Radtke, 2004). The estimation of MIS11 highstand sea level is also uncertain. This sea level highstand occurred between 398 and 410 ka ago, and its altitude is estimated to be close to the present sea level, within  $\pm 10$  m. Considering the older highstands, they have probably been lower than the present sea, and certainly not higher.

Here, three batches of experiments were performed with different sea level curves (Fig. 6): (1) the sea-level curve of Waelbroeck et al. (2002), starting the model at 400 ka; (2) the sea-level curve of Waelbroeck et al. (2002) between 0 and 430 ka, and that of Shakun et al. (2015) between 430 and 600 ka (named sea level curve “W+S”); (3) the sea level curve of Cutler et al. (2003) since 600 ka, modified with the sea level of Khan et al. (2017) determined from Caribbean data for the last 8 k.y. (named sea level curve “C+K”).

The three curves particularly take into account the fact that no sea level highstand is observed in the Caribbean during the Holocene. The different curves consider a MIS5e sea level at 6 m (Cutler et al., 2003, and Waelbroeck et al., 2002, respectively), which is close to the lowest sea level peak determined by Kopp et al. (2009). The curves also exhibit variabilities for the older sea level highstands (Siddall et al., 2007). The peaks altitudes differ by 5 m for MIS7b, 6 m for MIS9c, 11 m for MIS11, and 10–25 m for MIS15. Therefore, the different results of the models obtained with these three different curves

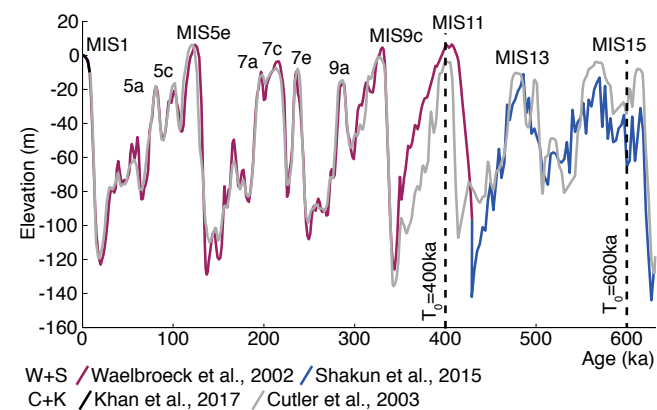


Figure 6. Sea-level curves used and tested by the reef growth models. See main text for description.



will describe the vertical motion history of Les Saintes in a most conservative way, taking into account sea level uncertainties. They are discussed in the Results section.

### **Maximum Reef Growth Rate (G)**

During the last transgression, reef accretion rate primarily determined whether a reef was able to keep growing with sea level rise (keep-up trajectory), to follow partially the sea level rise by retrograding along the coast (catch-up mode) or to be drowned (give-up growth trajectory, Neumann, 1985). Dullo (2005) reviewed the coral and Holocene reef growth rates measured in the Caribbean, and showed that the latter span 0.7–15.2 m/k.y., with an average rate of 6.1 m/k.y. (Dullo, 2005). The reef growth rate variability is greatly influenced by local hydrodynamic effects that influence for instance the distribution and development of coral species, and the erosion of the reef (see e.g., Barrett and Webster, 2017). Therefore, modeling the growth and morphology of the entire Les Saintes plateau with a high (>10 mm/yr) maximum reef growth rate is unrealistic. Recent considerations on the dependency of reef growth rate on water-depth also led several authors to review the Holocene reef growth rate in the Caribbean (Gischler, 2008; Hubbard, 2009) and found most of their measures fall below 4 m/k.y. Regarding these results, we used and tested maximum reef accretion rates between 0.5 and 10 m/k.y. in increments of 0.5 m/k.y.

### **Vertical Subaerial Erosion Rate (E)**

Estimating a vertical subaerial erosion rate is not straightforward. Few studies present weathering or karst erosion rates, and the few measurements that exist are not easy to link to vertical subaerial erosion rate. On Grand Cayman, Cayman Islands, Spencer (1985) used micro-erosion meters to measure weathering rates of the Pleistocene outcropping reef, and found a rate spanning 0.09–0.62 m/k.y. In northern Florida, USA, Opdyke et al. (1984) estimated a karst erosion rate from spring and seepage of  $\text{CaCO}_3$  to be between 0.026 and 0.08 m/k.y. These rates are of the same order of magnitude as subsidence rates discussed in the following section. Vertical subaerial erosion must therefore be taken into account in our models, and was added to the model presented in Toomey et al. (2013).

In the Guadeloupe archipelago, the MIS5e reef deposit outcrops on Marie-Galante and Grande-Terre islands are just 20 km east and northeast of Les Saintes archipelago (Battistini et al., 1986; Feuillet et al., 2004). The preservation of MIS5e and older Pleistocene terraces suggests quite low subaerial erosion rates. Consequently, models were run with reasonable values ranging between 0 and 0.15 m/k.y. in increments of 0.05 m/k.y., in agreement with the lower range of Grand Cayman weathering rates (Spencer, 1985) and with northern Florida karstic erosion rates (Opdyke et al., 1984).

### **Methodology to Constrain the Vertical Motion Rate (U)**

In order to explore and constrain the vertical motion history of Les Saintes, two different sets of models were designed and run: the 2-D model with constant vertical motion rate, and the model in its 1-D version with time-varying vertical motion rate.

In details, at first, we considered the simple assumption that vertical motion rate (U) is constant through time. Scenarios with a vertical motion positive (i.e., uplift) were tested, producing models with a morphology resembling the ones of uplifting islands, exhibiting staircase of fossil or erosive terraces (see Koelling et al., 2009, and Toomey et al., 2013 for several examples). However, on Les Saintes Islands, neither reef terraces nor erosion terraces are found onland. Even the well-developed MIS5e terrace found on the other islands of the archipelago (Table 1) is not outcropping. This indicates that the deformation is either of subsidence, or that no or slow deformation is accumulating and counterbalanced by a high subaerial erosion rate that would have washed away the reef deposits.

In this paper, we therefore only show results for values of U varied between 0 and  $-0.8$  m/k.y. in increments of 0.05 m/k.y. (refer to Koelling et al., 2009, and Toomey et al., 2013, for examples of models obtained with positive values of U). We ran more than 4000 models that generated synthetic reef morphology and stratigraphy, for different subaerial erosion rate, maximum reef growth rate, vertical motion rate, sea level history, basement shape, and start time, as described above. We analyzed every model outcome in order to identify the parameter combinations that generate the closest match to Les Saintes plateau. We extracted from the models the depths of the plateau and of the shallower surface of erosion ( $Z_{e1}$ ), in order to represent graphically the results over the model domain (e.g., Fig. 7). Results are described in the next section.

Second, we explored if and how the vertical motion rates can have varied through time in Les Saintes. In these tests, we used the model in its 1-D version, equivalent to model synthetic cores. They reproduce the reef stratigraphy taking into account reef growth (2.5, 5, and 7.5 m/k.y.), subaerial erosion (0.05 m/k.y.), the sea level history ("W+S"), a start time ( $T_0 = 330$  ka), an initial basement depth ( $z_0$  tested at 0, 75, and 150 mbsl), and a subsidence rate that can vary through time,  $U = f(t)$ . We tested 3 scenarios: (1) subsidence is constant through time (to compare and validate our approach with the 2-D models); (2) subsidence rate increases through time; (3) subsidence rate decreases through time. Linear and quadratic subsidence variations were tested. Results are presented in the last section of the following part.

## **RESULTS**

With a constant vertical motion rate, we explored the model outputs obtained for different parameter settings described above. At first, we only tried to reproduce the morphology of Les Saintes plateau, composed of a fringing reef and a drowned plateau.

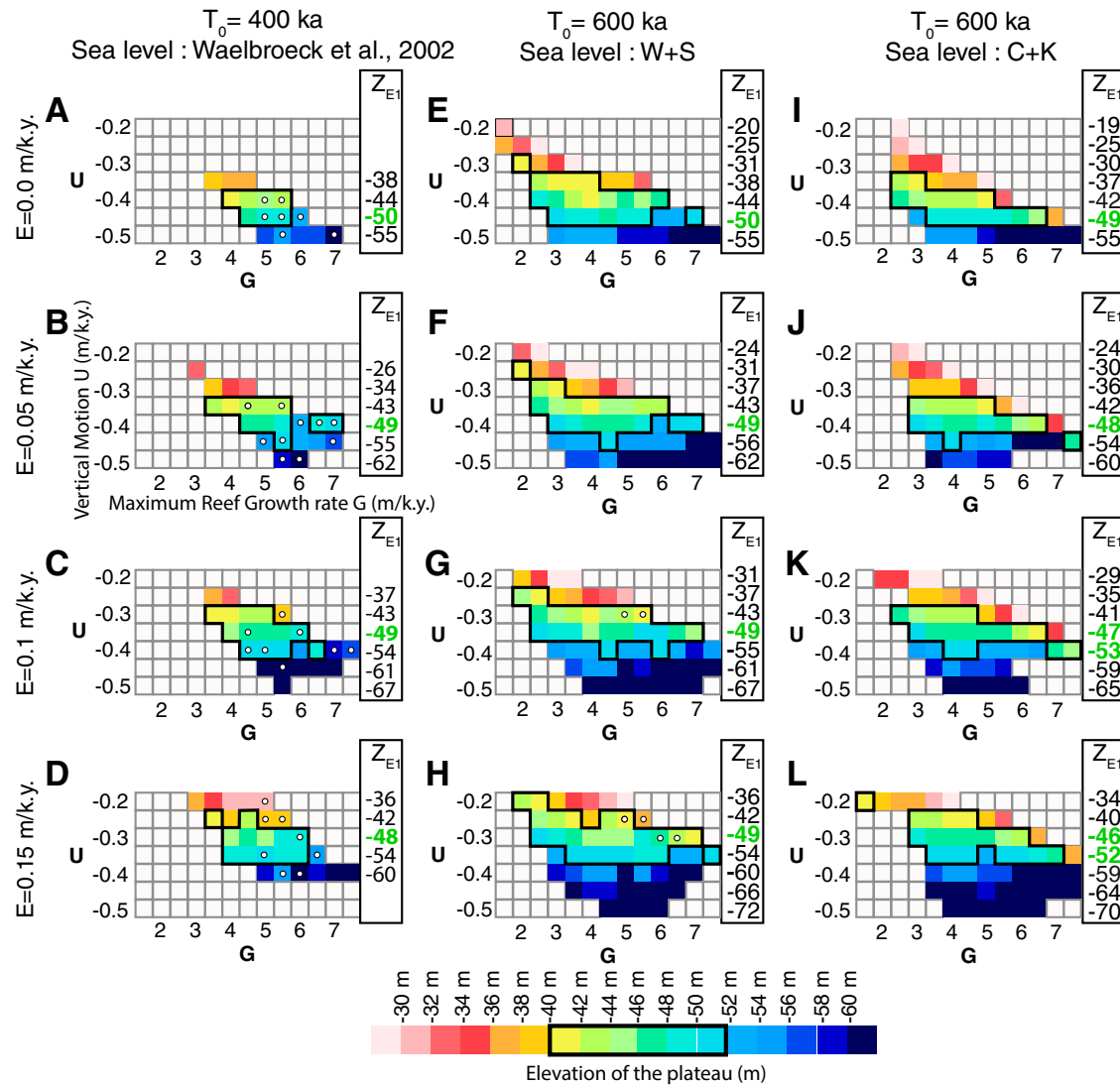


Figure 7. Variation of the elevation of the modeled plateau for different sets of parameters. For each plot, depth of the plateau is represented in color with regards to subsidence (U) and reef growth rate (G). Depths fitting with Les Saintes plateau are outlined in black, and depths of the shallower surface of erosion ( $Z_{E1}$ ) are indicated on the side. Columns: models run for different values of initiation time  $T_0$ , and for different sea level curves. Rows: models run for different values of subaerial erosion rates. Open white circles indicate models that present a double reef barrier along the seaward edge of the plateau. W+S—Waelbroeck et al., 2002, and Shakun et al., 2015; C+K—Cutler et al., 2003, and Khan et al., 2017.

## Modeling the Saintes Morphology

The morphology of the models mainly depends on the combination of two parameters: the reef growth rate  $G$ , and the subsidence rate  $U$ .

For a combination of slow reef growth (about  $G < 2.5$  m/k.y.) and high subsidence rates (about  $U < -0.4$  m/k.y.), the model produces a series of submarine reef terraces, looking like a drowned flight of stairs. In such a setting, the reefs are not able to keep up with relative sea-level rise through time, and give up quickly (see Supplemental Material<sup>1</sup> for examples, Fig. S1A). For a combination of high reef growth rates (about  $G > 6.5$  m/k.y.) and slow subsidence (about  $U > -0.25$ ), the model produces wide carbonate platforms that form plateaus similar to Les Saintes. However, they are systematically lying at present sea level (0 m), and not drowned at  $45 \pm 5$  mbsl (Fig. S1B). In this second setting, reef growth rates are high enough for reefs to keep up with relative sea level rise. Finally, for a combination of low reef growth and low subsidence, moderate reef growth and moderate subsidence, or high reef growth and high subsidence, the model reproduces a morphology close to that of Les Saintes: a drowned plateau generally associated with a fringing reef. Consequently, over the entire parameter domains, only a third of the models reproduced the “catch-up” morphology of the Saintes carbonate platform that we intend to compare to our bathymetry data (examples are shown in Figs. 8 and 9).

Figure 7 presents the compilation of the sensitivity tests carried out on different parameters, for a basement slope of 0.02 m/m. The models that were producing a fringing reef and a drowned plateau are represented in colored squares; color scale showing the depth of the drowned plateau (as indicated on Fig. 5). Next to each plot, a table indicates the depth of the first modeled surface of erosion at its intersection with the basement, marked  $Z_{E1}$  (indicated on Fig. 5) that will be compared with  $Z_{R1}$ , the depth of the reflector  $R_1$  (Fig. 3), close to the land, in a following section. Finally, open white dots are superimposed on the grid if the model output presents a double reef barrier along the seaward edge of the plateau (Fig. 7).

For combinations of reef growth and subsidence rates, the same trend is verified with the different vertical subaerial rates (Fig. 7, each row corresponds to a different erosion rate) as well as with the different start time ( $T_0 = 400$  ka in Figs. 7A–7D else  $T_0 = 600$  ka) and sea level curves used (Waelbroeck et al., 2002 in Figs. 7A–7D, “W+S” in Figs. 7E–7H, and “C+K” in Figs. 7I–7L).

Among these models, only a few can reproduce a plateau drowned at  $45 \pm 5$  mbsl (framed by black boxes in Fig. 7), the subsidence values span  $-0.2$  to  $-0.45$  m/k.y.

## Sensitivity Tests Analyses and Influence on the Vertical Motion Rate

Variability exists among the different models, depending on the parameter setting.

## Variability from Vertical Subaerial Erosion Rate

For any of the start times and sea level curves used, the vertical subaerial erosion rate influences the result as such: the more accommodation space is created by subaerial erosion during sea-level lowstands, the less subsidence is needed to model a drowned plateau. For  $E = 0$  m/k.y., closest-matches are modeled for  $-0.45 < U < -0.30$  m/k.y. (Figs. 7A, 7E, and 7I), while for  $E = 0.15$  m/k.y., closest matches are obtained for  $-0.4 < U < -0.2$  m/k.y. (Figs. 7D, 7H, and 7L).

## Variability from the Start Time $T_0$

A discrepancy is also seen when the models are starting at 400 ka (Figs. 7A–7D) or 600 ka (Figs. 7E–7L). If the model starts just before a high sea level highstand (as for  $T_0 = 600$  ka), the model will produce an aggrading deposit that can gain rapidly the shape of a plateau (see Fig. 9A, the deep brown isochrones have the shape of the plateau). Once this plateau shape is reached, the following deposits develop as flat units that stack vertically, and preserve the plateau shape of the carbonate platform.

On the contrary, if the model starts during a sea level drop (as for  $T_0 = 400$  ka), prograding deposits will form along the coast, as a staircase (see the brown deposits in Fig. 9C). From then, younger deposits will grow, aggrading and prograding (red to blue isochrones, Fig. 9C), to gain the shape of a plateau (see the dark blue and purple deposits, Fig. 9C). When a staircase morphology exists and persists, a double reef barrier can form along the seaward edge of the plateau (Fig. 9C; Fig. S2 [see footnote 1]). During the sea level rise following a sea level drop, reef built on the lower stair can keep up with sea level and form an outer barrier, while reef also develop on the upper stair and can form an inner barrier. Once both inner and outer barriers reach the same elevation, the reef gets a plateau shape.

Several hundreds of thousands of years can be needed for the reef to gain a plateau shape. On the entire model domain, when the start time is fixed at 600 ka (MIS15), the modeled platform usually gets a plateau shape very early (at 570 ka, as in Fig. 9A) or by maximum 400 ka. For models started at 400 ka, the plateau shape is reached only during MIS5. Therefore, on the entire model domain, for  $T_0 = 400$  ka, the couples of reef growth rate and subsidence rate able to produce the morphology of a drowned plateau are fewer (Figs. 7A–7C to compare with Figs. 7E–7J) but, the models presenting a double barrier are more numerous than for models started at 600 ka. The double barriers form when a stair exists in the morphology, and with reef growth rate high enough ( $> 4.5$  m/k.y.) for the reef on the lower stair to keep up with sea level rise. Figure 7 shows that for  $T_0 = 600$  ka, high erosion rate seems to be a requirement to promote double barrier development, and must modify enough of the morphology of the platform along its seaward edge to favor double barrier development (Figs. 7G, 7H).

For any  $T_0$ , the different models reproduce the same highest bound of subsidence rates:  $-0.45$  m/k.y. for  $E = 0$  m/k.y. (Figs. 7A, 7E, and 7I) and  $E = 0.05$

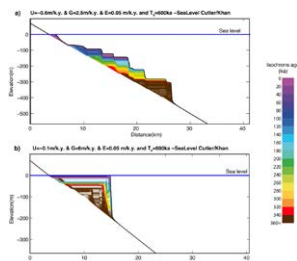
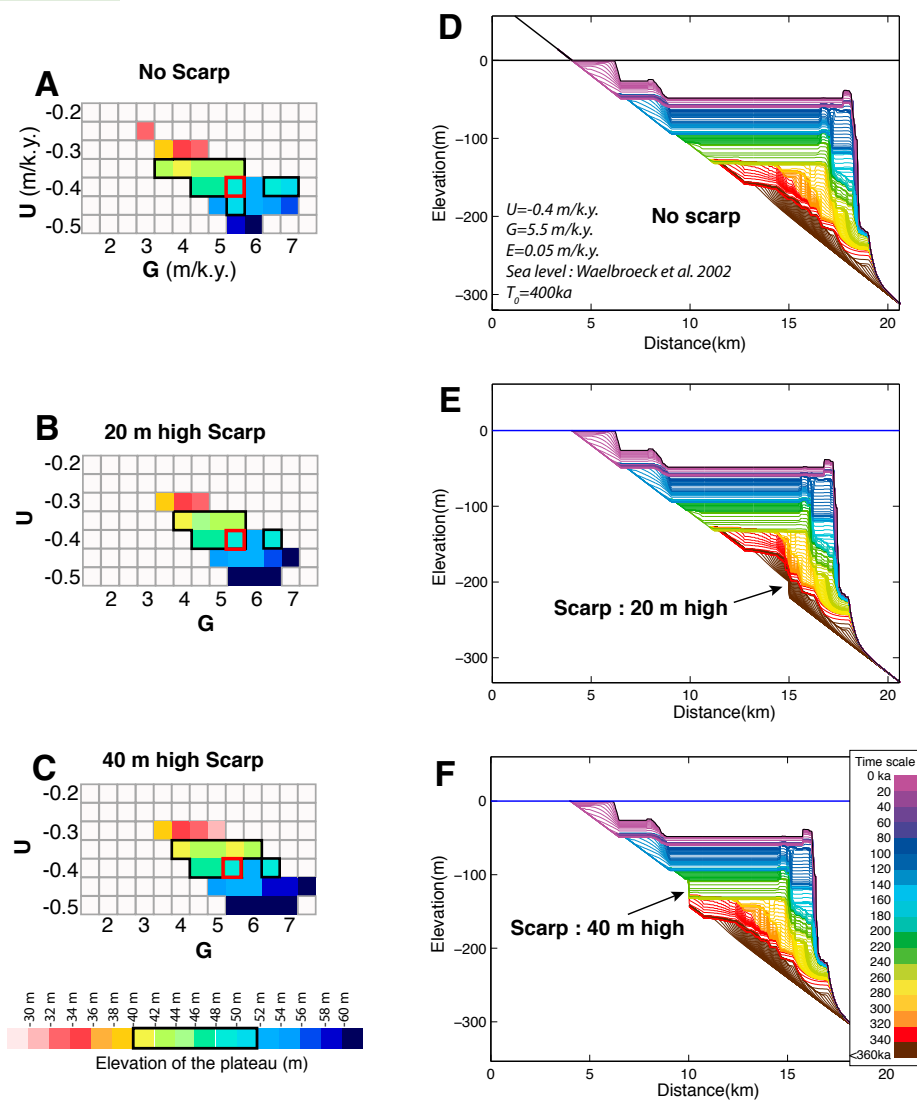


Figure S1. Examples of reef growth models that do not fit with Les Saintes carbonate platform morphology. (a) For low reef growth rates (0.5) and high subsidence rates (0.5), the model produces drowned reef deposits that have staircase morphology. This morphology corresponds for instance to the reef surrounding the island of Big Island, Hawaii. (b) For high reef growth rates and low subsidence rates, the model produces carbonate platform that have the shape of a plateau but that are not drowned, and instead are at the present sea level.

References:

Wentler, J.M., Briggs, J.C., Clague, D.A., Goffin, C., Hess, J.R., Potts, D.C., Remane, W., Ridgway, R., Blain, C., et al., 2009. Coral reef evolution on rapidly subsiding margins: Global and Hawaiian Chains. *PLoS ONE*, 4(10), 1–10. <https://doi.org/10.1371/journal.pone.0048703>.

<sup>1</sup>Supplemental Figures. Showing additional results obtained with the reef growth models. Please visit <https://doi.org/10.1130/GES02069.S1> or access the full-text article on [www.gsapubs.org](http://www.gsapubs.org) to view the Supplemental Figures.



**Figure 8.** Test on the modeled plateau's depth with regards to a linear basement shape (A) and the presence of faulting prior to reef growth (B, C). These models have been run with a subaerial erosion rate of 0.05 m/k.y., an initial time ( $T_0$ ) of 400 ka, and the sea level curve of Waelbroeck et al. (2002). (D, E, and F) show the internal stratigraphy of the platforms for different basement shapes and for a subsidence rate (U) of  $-0.4$  m/k.y. and a reef growth rate (G) of 5.5 m/k.y. The depths of the shallowest surface of erosion  $Z_{E1}$  are unchanged.

m/k.y. (Figs. 7B, 7F, and 7J),  $-0.4$  m/k.y. for  $E = 0.1$  m/k.y. (Figs. 7C, 7G, and 7K) and  $-0.35$  m/k.y. for  $E = 0.015$  m/k.y. (Figs. 7D, 7H, and 7L).

### Variability from Sea Level History

When all parameters are equal except the sea level curve, we can notice that models run with the composite sea level curve W+S (Figs. 7E–7H) produces overall good models for the same range of reef growth rates and subsidence rates than the models run with the composite sea level curve C+K (Figs. 7I–7L). A slight difference exists though; models produced with W+S curve can match the plateau's depth for smaller values of reef growth rates and subsidence rates. This is probably due to the fact that during the MIS7, MIS9c, and MIS11 the sea level is slightly higher in the W+S curve than in the C+K curve (Fig. 6). Therefore, less accommodation space is created during glacial periods when using the W+S curve, and the reef is better able to keep up with relative sea level rise during interglacial periods as the base level is higher.

These slight differences in rates of sea level change, and peaks of sea level during interglacial periods between the two curves used do also influence the presence or absence of double barriers, as the models run with the curve W+S generate a few models presenting double barrier along their seaward edge, while models run with the curve C+K do not.

### Influence of the Basement Morphology

Basement morphology can influence the growth and therefore the morphology of a reef carbonate platform, as it offers for the reef to develop wider or narrower surfaces (Cabioch, 2003). We tested the influence of the basement slope and shape on the reef models.

Models were run with two basement slopes of 0.02, and of 0.075, similar to the eastern and northwestern basement slope of Les Saintes plateau, respectively. We explored the different parameters in the model domain in order to reproduce the morphology of Les Saintes plateau. We found overall similar results: the model reproduces Les Saintes plateau's depth for intermediate values of reef growth rates and subsidence rates for both slope values.

In details though, for steeper basement, the model reproduces the plateau's depth for narrower ranges of reef growth and subsidence rates. Figure S3 (footnote 1) presents for instance a comparison of the model outcomes run with different slopes (slope of 0.02: Figs. S3A–S3D; slope of 0.075: Figs. S3E–S3H), during the last 600 k.y. with the sea level curve W+S, for different subaerial erosion rates. For a slope of 0.02, the models fitting Les Saintes plateaus' depth are obtained for reef growth rates G that spans 2–7.5 m/k.y. and subsidence rates between  $-0.2$  and  $-0.45$  m/k.y., while for a steeper slope of 0.075, G spans 2.5–7 m/k.y. and U spans  $-0.25$  to  $-0.45$  m/k.y.

We tested the influence of the presence of a scarp in the basement, in order to take into account the fault system that crosscuts Les Saintes plateau,

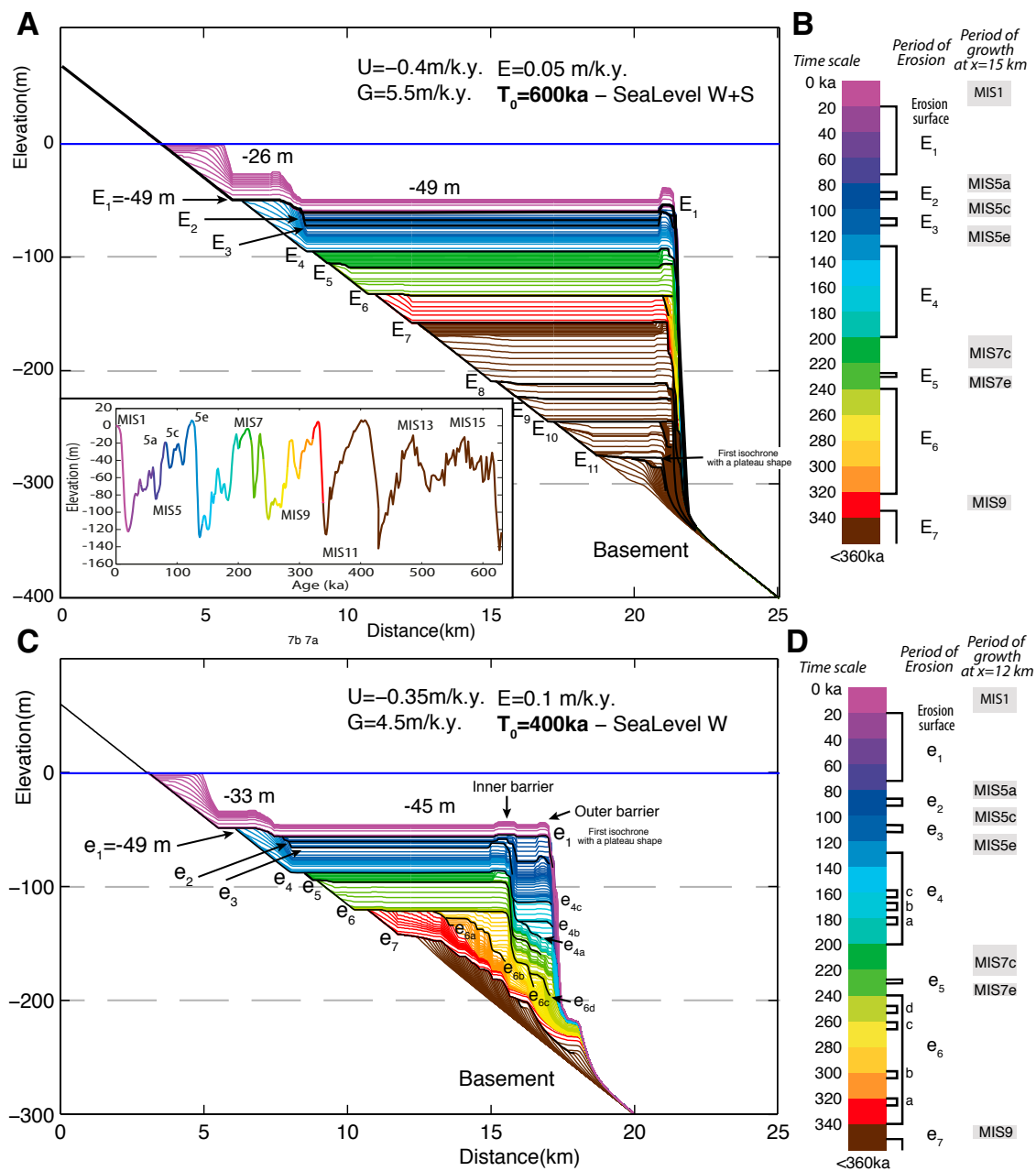


Figure 9. (A, C) Internal stratigraphy (1 k.y. isochrones) and (B, D) chronology of erosion and deposition of two of the best-fitting reef growth models for Les Saintes plateau, Guadeloupe, French West Indies, for different  $T_0$ . (A) The model is obtained with an initial time  $T_0 = 600 \text{ ka}$ , slope = 0.02, maximum reef accretion rate of 5.5 m/k.y., subaerial erosion rate of  $-0.05 \text{ m/k.y.}$  and vertical motion rate of  $-0.4 \text{ m/k.y.}$ , and modeled with the W+S sea level curve colored in the inset (Waelbroeck et al., 2002 and Shakun et al., 2015). (C) The model is obtained with an initial time  $T_0 = 400 \text{ ka}$ , slope = 0.02, maximum reef accretion rate of 4.5 m/k.y., subaerial erosion rate of  $-0.1 \text{ m/k.y.}$  and vertical motion rate of  $-0.35 \text{ m/k.y.}$ , modeled with the sea level curve of Waelbroeck et al. (2002). Black lines: Erosion surfaces, numerated (E or e) formed during period of erosion indicated in (B) and (D).

and whose activity is older than the reef construction (Leclerc et al., 2016). As their slip rates are very likely to be one order of magnitude smaller than the reef growth rates, we did not model the scarp growth through time. We modified the linear basement shape and added a 20-m-high and a 40-m-high scarp, at different places along the basement. Models reproduced Les Saintes plateau's depth and the depth of the shallower erosion surface  $Z_{E1}$  for the same ranges of parameters with or without faults (Fig. 8). The presence of a scarp influences the reef growth structure around the scarp but as sea-level highstands have amplitudes of  $\sim 120$  m, that is 3–6 times the height of the scarps, it seems not to influence much the overall morphology of the platform.

These different tests allow us to be confident in the range of the parameter values, and in particular in the subsidence rate range, needed to model Les Saintes reef plateau, for reasonable basement slopes and shapes.

### Modeling the Saintes Carbonate Platform Structure

One way to tighten our estimation of the subsidence rate in which a carbonate platform such as Les Saintes plateau formed is to use the structure of the platform as a constraint. In particular, we can use the depth  $Z_{R1}$  of the reflector  $R_1$  close to the land as a marker of the deformation. Reflector  $R_1$  is a surface of erosion. The intersection of  $R_1$  and the basement is similar to the inner edge (or shoreline angle) of uplifted terraces that mark the highest level of the sea at the time of formation of the terrace (e.g., Lajoie, 1986; Armijo et al., 1996). This marker is therefore a relevant marker of the vertical deformation of a coast. Onland, in uplifting context, inner edges can be easily identified on topography, as it consists of slope breaks. On the contrary, offshore, and in such subsiding context, reef units are vertically stacked, and the inner edges are hidden by and buried under the subsequent reef growth. Therefore, accessing inner edge depth is only possible using seismic reflection profiles. In our seismic data, we do not image the contact of the reef deposits with the basement. However, we do image  $R_1$  at only a few hundreds of meters from the island coasts, lying at  $49 \pm 4$  mbsl, considering a velocity of 1500–3000 m/s in the backreef. Without more information, we can only hypothesize that the inner edge of the seismic unit SU2 is presently at a maximum depth of  $\sim 49 \pm 4$  mbsl.

We measured the depth of the first surface of erosion  $Z_{E1}$  identified under the post-LGM deposit in the models, where it intersects the basement. We compared  $Z_{E1}$  to  $Z_{R1}$ . Values matching  $49 \pm 4$  mbsl are marked in green on Figure 7. We can notice that the modeled inner edge depth can vary greatly in the model domain, but matches the  $49 \pm 4$  mbsl for subsidence rates in the range of  $-0.3$  to  $-0.45$  m/k.y.

By combining both criterions: (1) a modeled plateau at  $45 \pm 5$  mbsl and (2)  $Z_{E1}$  at  $49 \pm 4$  mbsl, and analyzing the entire set of models, we propose that Les Saintes reef plateau morphology and structure can be modeled in a subsidence context, with a subsidence rate of  $-0.3$  to  $-0.45$  m/k.y.

### Description of the Best-Fit Results

Figure 9 represents two of our best-fit models, obtained for initial times of 600 and 400 ka. They were obtained for a constant subsidence rate of  $-0.4$  and  $-0.35$  m/k.y., a reef growth rate of 5.5 and 4.5 m/k.y., a subaerial erosion rate of 0.05 and 0.1 m/k.y., respectively. The models are composed of several stacked sediment packages separated by erosion surfaces, drawn in black and named  $E1/E11$  and  $e1/e7$ , respectively.

The bathymetric profiles of both models are close to the profile of Les Saintes plateau (Fig. 2A). The modeled platform obtained with  $T_0 = 600$  ka presents a fringing reef, a small terrace at 26 mbsl, a wide plateau drowned at 49 mbsl and a 10-m-high barrier along the edge of the plateau. The other model, obtained with  $T_0 = 400$  ka also present these features: a fringing reef, a small terrace at 33 mbsl, a wide plateau drowned at 45 mbsl. Furthermore, it shows a 4-m-high double barrier built along the edge of the plateau, similar to the one seen in the bathymetric data (Leclerc et al., 2014).

Both models share common history. The shallower unit is the post-LGM deposit (MIS1, in purple) that built on top of the MIS5 deposits (in blue). The post-LGM unit deposited on a surface of erosion  $E_1/e_1$  that lies at 49 mbsl close to the island and deepens seaward to 59 mbsl. This surface constitutes the upper bound of the MIS5 reef units. Overall, the MIS5 deposit is almost 40 m thick and presents two inner erosion surfaces,  $E_2/e_2$  and  $E_3/e_3$ , which result from sub-stages sea level lowstands, during MIS5b and MIS5d, respectively. Below, the MIS7e and MIS7c are stacked vertically (in green) over either the horizontal reef unit built during MIS9 (in red, Fig. 9A) or, above prograding reef units built between MIS9 highstand and MIS8 lowstand (red to yellow, Fig. 9C).

When comparing these models to the seismic profiles we described above (Figs. 3 and 4), the seismic unit SU1 corresponds to the post-LGM deposit, and the reflector  $R_1$  corresponds to the erosion surface  $E_1/e_1$  that formed through the LGM period. As no age controls are available to constrain the age of the deeper seismic units, we cannot validate the stratigraphy at depth that is modeled here. We can only note that above 90 mbsl, three surfaces of erosion are imaged in the seismic profiles, and three surfaces of erosion are modeled. For reasonable and constant reef growth rate, subaerial erosion rate, and subsidence rate, the deeper seismic units SU2, SU3, and SU4 could correspond to the reef deposited during the substages of MIS5, and  $R_2$  and  $R_3$  could be related to erosion during the MIS5 sub-stages sea level lowstands, here  $E_2/e_2$  and  $E_3/e_3$ , respectively.

### Exploring Possible Subsidence Rate History

With the first sets of models described above, we showed that Les Saintes plateau morphology and stratigraphy can be modeled in a context of subsidence, and for constant subsidence rates of  $-0.3$  to  $-0.45$  m/k.y., since at least the last-glacial maximum (i.e., time of  $R_1$  formation). Coring and isotopic or biostratigraphic dates as well as deeper seismic reflection imaging are needed

to constrain the deep structure of Les Saintes plateau, as well as its entire vertical motion history, that might have varied through time. For comparison, the nearby islands of Marie-Galante and La Désirade underwent uplifts that slowed down during Upper-Pleistocene (Feuillet et al., 2004, Léticée et al., 2019). Being aware of our lack of constraints on the subsidence history of Les Saintes, we therefore propose to simply test if Les Saintes plateau can have formed in a context of subsidence that has slowed down or accelerated through time.

As described above, we used the reef model in its 1-D version, and modeled reef accretion along a subsiding coast, whose subsidence rate is a function of time. As discussed earlier, the start time of the model does not affect much the upper section of the plateau (only the presence or absence of double barriers), where we have seismic stratigraphic constraints. Moreover, as we can notice in Figure 10, Figure S4 (footnote 1), and similarly to the results of our best fit 2-D model (Fig. 9), the seismic units are associated in these models to MIS5 substages reef deposits only. Therefore, for these reasons we set up our model starting only 330 k.y. ago. Figure 10 shows the results of these models for  $z_0 = 75$  mbsl, a reasonable initial basement depth that allows us to compare the synthetic cores with the Les Saintes plateau stratigraphy, seaward of the 25 mbsl terrace, below the 45 mbsl plateau.

On Figure 10, the synthetic cores are represented as a function of subsidence rates, colored by reef age. Surfaces of erosion are plotted as black dots, and are named  $E_i$  only when cited in the text. For comparison, we superimposed the Saintes plateau's depth (pink horizontal bar), as well as the depth's range of the three reflectors  $R_1$ ,  $R_2$ , and  $R_3$  (represented as colored boxes at 52–71 mbsl, 63–90 mbsl, and 76–109 mbsl, respectively). We consider a synthetic core compatible with our data when it is  $45 \pm 5$  mbsl deep, and presents at least two surfaces of erosion, each within the depth domains of  $R_1$ , and  $R_2$ , i.e., falling in the colored boxes ( $R_3$  is also represented for reference). Table 4 summarizes the results of the three vertical motion history scenarios.

First, we modeled the synthetic cores for a constant subsidence rate (Figs. 10A–10D), in order to compare with our 2-D simulations. We obtained cores compatible with the data for reef growth rates of 5 and 7.5 m/k.y., and subsidence rates of about  $-0.4$ , and about  $-0.55$  m/k.y., respectively (Figs. 10B, 10C). For  $G = 5$  m/k.y., this is in very close agreement with the 2-D models. For  $G = 7.5$  m/k.y., the 1-D model produces a plateau at  $45 \pm 5$  mbsl, while the 2-D simulations produce a plateau much deeper ( $>60$  mbsl, Fig. 7B). This discrepancy is probably due to the fact that reef growth rate decreases horizontally in the 2-D simulation, away from the open-sea, a process that is certainly critical on reef morphology for such a reef growth rate. For  $G = 2.5$  m/k.y. (Fig. 10A), we modeled a synthetic core at a depth of  $45 \pm 5$  mbsl, for a subsidence rate of about  $-0.2$  m/k.y., however, the stratigraphy does not match our data, as the erosion surface  $E_2$  is deeper than the depth range of  $R_2$ . Synthetic cores modeled with  $G = 10$  m/k.y. show systematically a surface of erosion  $E_i$  deeper than  $R_1$  (Fig. 10D).

Using a subsidence rate that increases linearly from 0 m/k.y. at 330 ka to  $U$  at 0 ka (Figs. 10E–10H), the model produced a good stratigraphy for low reef growth rates. With  $G = 2.5$  m/k.y., we obtained 4–5 stacked units for a

final subsidence rate close to  $-0.2$  m/k.y. (Fig. 10E). However, the upper deposit (equivalent to SU1) is only a few meters thick, that is not realistic as not comparable with our seismic profiles. With  $G = 5$  m/k.y., we also obtained a core presenting 4–5 vertically stacked units, with reasonable thicknesses, for a final subsidence rate of about  $-0.27$  m/k.y. (Fig. 10F). For higher reef growth rates (Figs. 10G, 10H),  $E_1$  or  $E_2$  are too deep in the few models that generate synthetic cores at appropriate depths.

Using a subsidence rate that decreases linearly from  $U$  at 330 ka to 0 m/k.y. at 0 ka, the model generated a reasonable stratigraphy only for  $G = 2.5$  m/k.y. and  $U = -0.26 \pm 0.01$  m/k.y. However, the upper unit is again only a few meters thick, which does not correspond to the observations made along the seismic profiles. When using higher reef growth rates, the reef is able to keep up with sea level, and a plateau forms at sea level.

We also tested a quadratic function for subsidence variations that showed the same trend (Fig. S4 [footnote 1]): for models with decreasing subsidence through time, no appropriate cores were modeled (Figs. S4E–S4H), while for subsidence rate increasing through time, several parameters combinations reproduce the stratigraphy: (1) for  $G = 2.5$  m/k.y., cores were compatible for final  $U$  of  $-0.28 \pm 0.01$  m/k.y., but the upper unit is only a few meters thick (Fig. S4A); (2) for  $G = 5$  m/k.y., cores were good for final  $U$  of  $-0.24 \pm 0.01$  m/k.y. (Fig. S4B); (3) for  $G = 7.5$  m/k.y., cores were compatible with data for final subsidence of about  $-0.26$  m/k.y. (Fig. S4D).

Therefore, these tests tend to indicate that if subsidence has varied through time (here modeled since 330 ka only, as we lack information about the deep stratigraphy of the plateau) subsidence may have increased rather than decreased recently. Further tests and age constraints are required to confirm such a trend.

## DISCUSSION

This reconstructed accretion history of Les Saintes reef plateau offers a new perspective on long-term deformation along the Lesser Antilles volcanic arc. The morphological and structural agreements between the geophysical data imaging the reef plateau and the models of late Quaternary plateau growth indicate that the archipelago has experienced a subsidence that we are able to quantify. All the models performed and presented above, for any sea level curve, basement morphology, range of appropriate reef growth rates, and subaerial erosion rates show that Les Saintes plateau cannot be modeled in neutral tectonic context, but in subsiding context only. Interpretation of these models implies that the subsidence rate, if constant through time, is of the order of  $-0.3$  to  $-0.45$  m/k.y., and if varying through time, is probably increasing to about  $-0.2$  m/k.y. since several hundreds of thousands of years (modeled here since 330 ka only).

While Leclerc et al. (2014, 2015) had suggested subsidence in Les Saintes and in Martinique, along the volcanic arc, this study confirms this vertical motion history, in Les Saintes.

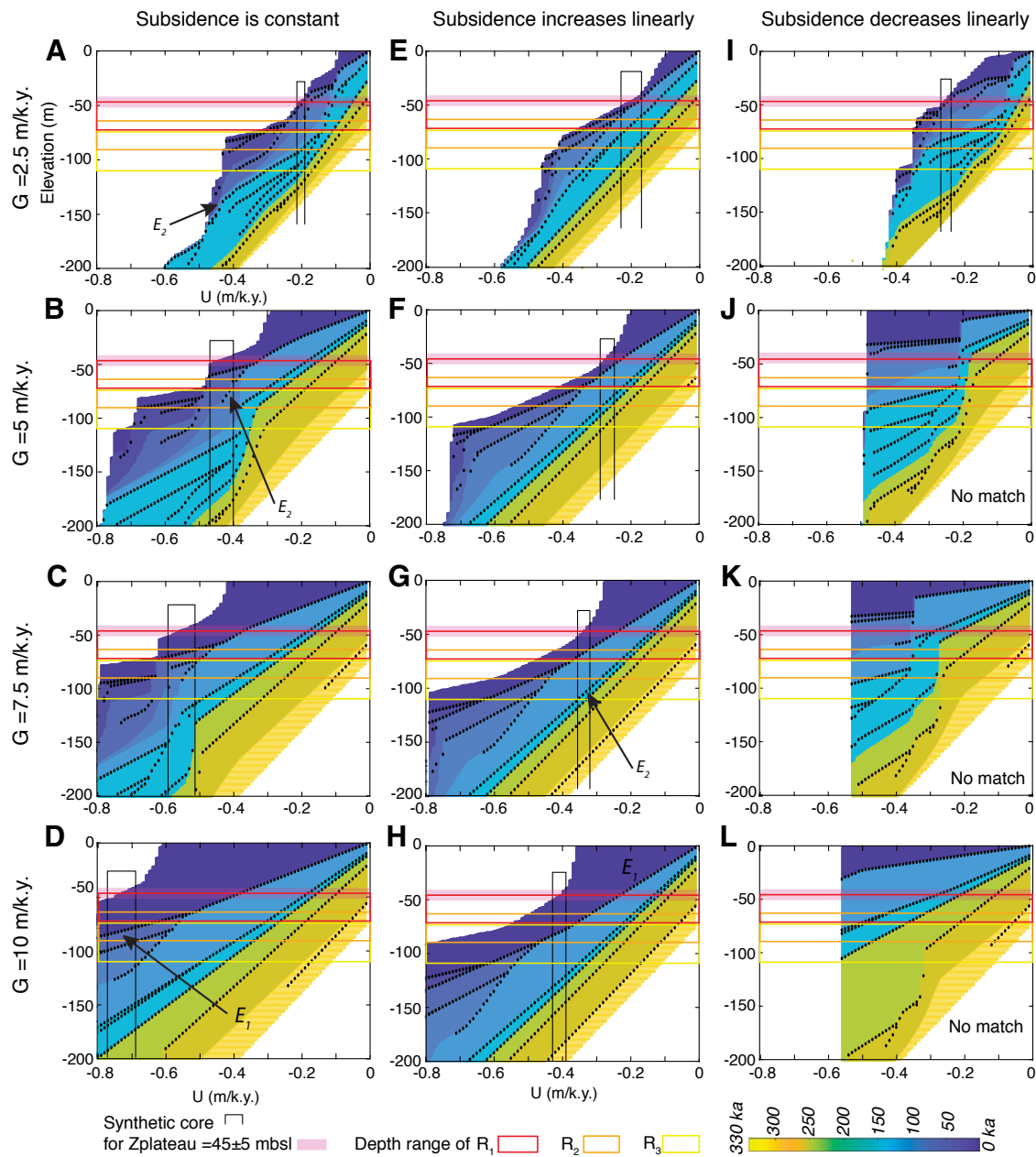


Figure 10. 1-D modeling producing stratigraphy of synthetic cores as a function of subsidence rates (U) for different reef growth rates (G). Subsidence can be constant (A–D), can increase linearly through time from 0 m/k.y. to U (E–H) or can decrease linearly through time from U to 0 m/k.y. (I–L). Deposits are colored by age. Surfaces of erosion are represented as black dots. Superimposed on the synthetic cores are benchmarks to compare with the geophysical data: pink box represents the depth of Les Saintes plateau at  $45 \pm 5$  mbsl, the red square indicates  $R_1$ 's depth: 45–71 mbsl; the orange box indicates  $R_2$ 's depth: 63–90 mbsl; the yellow box represents  $R_3$ 's depth: 76–109 mbsl. Black bars indicate synthetic cores that are at depths comparable with Les Saintes plateau's depth.  $E_1$  and  $E_2$  are surfaces of erosion cited in the main text.



TABLE 4. RESULTS OF THE 1-D MODEL EXPERIMENTS, WITH VARIATION OF SUBSIDENCE RATES, AT  $z_0 = -75\text{m}$

Mathematic function used to model subsidence	Growth rate (m/k.y.)	Subsidence (U) to model appropriate plateau's depth (m/k.y.)	Comments on the modeled plateau structure above 110 mbsl	Match the plateau architecture?
Constant	2.5	-0.19 to -0.20	Shallow unit too thin, E2 too deep	No
	<b>5</b>	<b>-0.4 to -0.47</b>	<b>4 units, E2 too deep for <math>U &lt; -0.42</math></b>	<b>Yes, <math>U = -0.41 \pm 0.01</math></b>
	<b>7.5</b>	<b>-0.53 to -0.59</b>	<b>4 units, E2 too deep for <math>U &lt; -0.56</math></b>	<b>Yes, <math>-0.51 \leq U \leq -0.56</math> m/k.y.</b>
	10	-0.70 to -0.77	E1 is too deep (>80 mbsl)	No
Increases linearly from 0 to U	2.5	-0.17 to -0.22	4–5 units, shallowest unit too thin	Yes
	<b>5</b>	<b>-0.26 to -0.28</b>	<b>4 to 5 units</b>	<b>Yes</b>
	7.5	-0.32 to -0.35	E2 is too deep (>100 mbsl)	No
	10	-0.39 to -0.43	E1 is too deep (>80 mbsl)	No
Decreases linearly from U to 0	2.5	-0.26 ± 0.01	4 units, shallowest unit too thin	Yes
	5	—	Plateau is modeled at 0 mbsl	No
	7.5	—	Plateau is modeled at 0 mbsl	No
	10	—	Plateau is modeled at 0 mbsl	No

Note: Plateau depth:  $45 \pm 5$  m; R1 depth: 45–71 mbsl; R2 depth: 63–90 mbsl; R3 depth: 76–109 mbsl. mbsl—meters below sea level. Parameter combinations that reproduce Les Saintes plateau architecture and an appropriate thickness for the post–Last Glacial Maximum unit are in bold. — indicates that none of the parameters tested produced a stratigraphy similar to Les Saintes plateau.

### Spatial Distribution of the Long-Term Vertical Deformation in the Guadeloupe Archipelago

#### Since 125 ka

Battistini et al. (1986) notice that the terrace formed during the MIS5e highstand (125 ka), when the sea level was +6–9 m above the current sea level (Kopp et al., 2009, Dutton and Lambeck, 2012), is present along the coasts of La Désirade, Marie-Galante, and eastern Grande-Terre, but is absent along the coasts of Basse-Terre, Les Saintes, and southwestern Grande-Terre (see Table 1, Battistini et al., 1986, Bouysse et al., 1993, Feuillet et al., 2004, Lardeaux et al., 2013, Weil-Accardo, 2014, Léticée et al., 2019). Where outcropping on land, its inner edge (also named shoreline angle) lies at different altitudes between 2–3 m and 10 m, decreasing from east to west (Table 1; Figs. 11A, 11B).

The islands are crosscut by several normal faults that have scarps of a few tens of meters. They can locally deform the terraces (through tilting and elastic flexure). The altitude of the shoreline angle of the terraces (in Table 1) are obtained in areas far from or not affected by recent fault activity (La Désirade, northern Grande-Terre, Battistini et al., 1986), or corrected from offset and elastic flexure (in Marie-Galante, Feuillet et al., 2004). The westward lowering of the MIS5e terrace is therefore not related to local faulting.

Since 125 ka, the coasts of La Désirade and east Marie-Galante are accumulating no or slow deformation (uplift of 1–4 m considering a sea level at 6–9 m 125 ka ago). The coast of east Grande-Terre either does not accumulate deformation, or very slowly subsides (3–4 m considering a MIS5e highstand at 9 m). Finally, the western coasts of Marie-Galante and Grande-Terre are slowly subsiding, by a few meters (maximum 7 m) since MIS5e. On the forearc islands, vertical motion rates are therefore very slow since 125 ka, on the order of  $10^{-3}$ – $10^{-2}$  m/k.y. only.

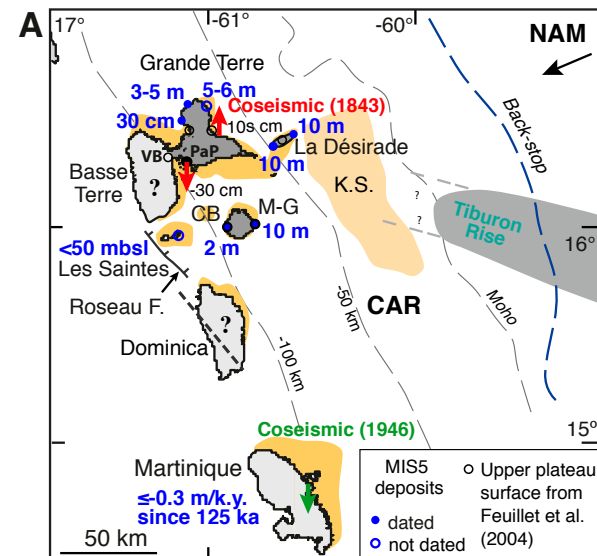
The seismic profiles across Les Saintes plateau show that the shallowest surface of erosion, associated here with the top of the MIS5e deposit, is deep, and at most 50 mbsl deep ( $Z_{R1}$ ) close to the shore. Therefore, the altitudes of the MIS5e deposits show a westward deepening along the Guadeloupe archipelago, particularly strong in Les Saintes, with a vertical motion rate an order of magnitude higher than the ones of the forearc islands (Figs. 11A, 11B).

#### Over Longer-Time Scales

In the Guadeloupe forearc, along the coasts of Marie-Galante, La Désirade, and Grande-Terre islands, quaternary reef deposits outcrop on land at several tens of meters above sea level and the MIS5e deposit. They can form flights of reef terraces surrounding high plateaus formed by Plio–Pleistocene carbonate platform deposits (Andreieff et al., 1989; Cornée et al., 2012; Münch et al., 2014).

The forearc islands share a similar morphological asymmetry: they can exhibit steep cliffs in the east, and mangroves in the west, and more terraces along their eastern coasts than along the western ones. The terraces are tilted to the west in Marie-Galante, by a few tenths of a degree, the older the terrace the more (Feuillet et al., 2004). The topography of the upper plateaus of Marie-Galante and north Grande-Terre show that they are also tilted to the west (Table 2). To the east, the upper plateau of La Désirade, though tilted to the north, is located at the highest altitude (276 m, Table 2), while the same carbonate platform is found at -79 m to the west, in eastern Basse-Terre, beneath volcano-clastic deposits (Versaille Borehole located in Fig. 11A, Garrabé and Paulin, 1984). This evidence led Feuillet et al. (2004) to propose that the upper plateaus of the forearc islands emerged at the same time and were tilted subsequently to the west, overall by  $\sim 0.35^\circ$  (if projected along a transect perpendicular to the subduction, Fig. 11C). More recently, Münch et al. (2013)

Figure 11. Pattern of the upper Pleistocene deformation of the Lesser Antilles. (A) Regional distribution of the MIS5 reef deposits over Guadeloupe archipelago and French West Indies (see also Table 1). NAM—North American plate; CAR—Caribbean plate; mbsl—meters below sea level; VB—Versaille Borehole; PaP—Pointe-à-Pitre; CB—Colombie Bank; M-G—Marie Galante; K.S.—Karukera Spur. Blue dots show dated reef deposits, while open blue dots show inferred MIS5 reef deposits. Elevation and references indicated in Tables 1 and 3. Roseau fault simplified trace in gray (after Leclerc et al., 2016). Vertical motion rates of the coasts of Martinique after Leclerc et al. (2015). Red arrows: coseismic deformation during the 1843 earthquake (after Sainte Claire Deville, 1843). Green arrow: coseismic deformation during the 1946 Martinique earthquake (Weil-Accardo et al., 2016). Submarine reef platforms are in orange. Back-stop and iso-depths of the plate interface as in Figure 1, after Paulatto et al. (2017). (B) Elevation of the MIS5 reef deposits along a transect perpendicular to the subduction. Data are presented in Table 1. The red bar represents the depth of  $R_1$ , the shallower surface of erosion identified in the seismic profile, calculated near the coast ( $49 \pm 4$  mbsl). Location of normal faults that could influence the altitude of the deposit in green dashed lines. (C) Elevation of the surface of the upper plateau (black open dots in section A), along a transect perpendicular to the subduction, modified after Feuillet et al. (2004). Red dot and error bar: depth range of the MIS9 reef deposit extracted from our best models of Les Saintes carbonate platform, red dot corresponds to the model of Figure 9, in the scenario assuming that the surface of the Plio–Pleistocene upper plateaus emerged 330 k. y. ago, see text for discussion. Normal faulting offsets and induced elastic flexure are either corrected or are accounted for within the error bars (size of the dot) in the plot, except in La Désirade where the Coulée du Grand Nord fault (in green dashed lines) offsets the upper-plateau by ~100 m. This induces that the upper-plateau located on the footwall side of the normal fault was uplifted due to faulting only by 20 to 30 m at most, considering that the ratio of footwall uplift with regards to hanging wall subsidence is equal to 0.5–1.3.5 (Stein et al., 1988; Armijo et al., 1996; Ford et al., 2012). The Roseau fault system is also shown nearby Les Saintes, in green dashed lines.

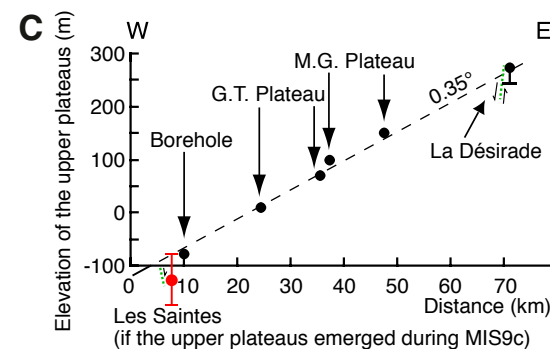
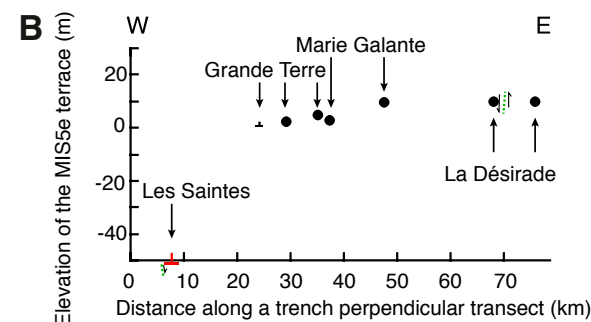


imaged the seismic stratigraphy of the submerged Colombie Bank, a 45 mbsl carbonate bank composed of Quaternary sedimentary units, located between Les Saintes, Basse-Terre, and Marie-Galante islands (Fig. 1). This bank has recorded subsidence and also probably the westward regional tilt, as the deeper (and older) the seismic unit, the more tilted it is.

In Les Saintes, we did not evidence a clear tilt of the stratas in the seismic profiles (Figs. 3 and 4, Leclerc et al., 2014). This could mean either that there is none, or that it is very small ( $<0.1^\circ$ ) and not identifiable in our seismic data (the seismic lines are not converted to depth profiles). The shoreline angles of the reef units, a marker formed horizontal at its time of formation, are hidden by subsequent reef growth, preventing us from determining any tilt.

In Marie-Galante and Grande-Terre, Feuillet et al. (2004) dated several samples from higher terraces (Table 2) and showed that the uplift rates were of the order of  $10^{-1}$  m/k.y. since MIS7 (ca. 250 ka), higher than the one estimated since 125 ka. Lécécie et al. (2019) also dated terraces in La Désirade, and estimated a minimum uplift rate of the order of  $10^{-1}$  m/k.y. since  $306 \pm 6$  ka that shows that the uplift rate has also slowed down through time. We have tested how the vertical motion of Les Saintes plateau might have changed through time. The results of our modeling tend to show that if so, subsidence has increased since the last hundreds of thousands of years. If all these transient deformations are linked, this could imply large scale transient processes occurring probably along the subduction interface and at depth.

From morphological considerations and correlation of the upper plateau and terraces of Marie-Galante with the SPECMAP curve, Feuillet et al. (2004) also propose that the upper plateaus, although formed earlier, emerged at the



same time, around 330 ka and were subsequently tilted uniformly westward, away from the trench. Following this scenario, we calculated that if Les Saintes plateau was to follow the same tilt, MIS9c deposit should stand at ~80 mbsl (Fig. 11B). As acknowledged above, we cannot constrain the deep structure of Les Saintes plateau, lacking information of the deep deposits' ages. However, we can note from the different 2-D reef growth models, i.e., in a context of constant subsidence over the past sea level highstands, that for models that can reproduce both the morphology and the depth of the first surface of erosion, the modeled MIS9c surface is found between 80 and 175 mbsl. Only three models show a MIS9c at 80 m, for reef growth rates  $\leq 2.5$  m/k.y. and weak subsidence rates ( $\leq -0.25$  m/k.y.). In other cases, MIS9c is modeled much deeper.

On the basis of biostratigraphy of calcareous nannofossils and planktonic foraminifera, datings of volcanic deposits found within the carbonate deposits, and magneto-stratigraphy analysis of the carbonate sequence performed on Grande-Terre (Münch et al., 2014 and references therein) showed that the upper carbonate platform sequence of the "upper plateaus" of the forearc islands formed between ca. 1.07–1.48 Ma, and proposed that they emerged in the same time span, much earlier than Feuillet et al. (2004). In such cases, Léticée et al. (2019) estimate that since 1.07–1.48 Ma, the uplift rate of La Désirade (and by extension of Marie Galante) has decreased gradually through time, from  $10^{-1}$  m/k.y. at the time of emergence, to  $10^{-3}$  m/k.y. since 125 ka. All authors agree that uplift rates have decreased through time (either from 1.07 to 1.48 Ma or from 330 ka, Münch et al., 2014 and Feuillet et al., 2004, respectively).

In comparison with other islands, Les Saintes archipelago seems to be vertically deforming at a quite (and increasing?) fast rate, over at least the past 125 ka. Our results suggest that westward constant tilting alone is not sufficient to promote deformation in Les Saintes (Figs. 11A–11C).

### Processes Driving Deformation in the Upper Plate

Les Saintes plateau is located along a volcanic arc, in a tectonically active area. Its subsidence can therefore be driven by volcanic processes and local tectonic activity induced by the regional fault system, as well as by subduction related processes, the contribution of these processes is discussed below.

### Volcanic Activity Influence

There are three mechanisms linked to volcanic processes that could promote deformation in the upper plate.

While cooling, magma chambers can generate subsidence. Thermal subsidence rate is typically an order of magnitude slower than the rate estimated in Les Saintes (Grigg, 1997). Tallarico et al. (2003) also show that thermal subsidence decreases rapidly with time, in a few tens of thousands of years. As the volcanic activity in Les Saintes stopped by 800 ka (Zami et al., 2014), the thermal subsidence is certainly weak, if not absent, at least since 125 ka.

Battistini et al. (1986) proposed that the pattern of the deformation in the Guadeloupe forearc could be due to volcano-isostatic effects promoted by the building of the Basse-Terre volcanoes. Indeed, the load by a volcano of an elastic lithosphere induces its flexure, manifested as a deep deflection and a small positive forebulge on the deflection's edge (e.g., around the Big Island in Hawaii, USA, Walcott, 1970; Moore, 1970). We tested this hypothesis by calculating the equivalent elastic thickness of the plate necessary to generate the pattern of the MIS5e deformation (see Appendix). This calculation does not require to estimate neither the volume of the island nor the forces applied by the load on the plate. We found that the elastic thickness of the plate would be 7–13 km, a value whose lower bound is close to the elastic thickness estimated at 5 km by Feuillet et al. (2004) from modeling of fault elastic flexure in Marie-Galante.

Despite this result, several arguments tend to show that such mechanism is not responsible for the deformation observed in the Lesser Antilles. For instance, the amount of uplift of a forebulge induced by the loading of an elastic plate is two orders of magnitude smaller than the amount of deflection below the load (Walcott, 1970; Fowler, 2004). If it seems to be the case in Guadeloupe since 125 ka, on longer time scales it is not. The altitude of the upper plateaus of east Marie-Galante and La Désirade are much higher than the altitude of the same unit in the Versailles borehole next to the volcanic complexes (Table 2). Furthermore, a deflection should also exist west of the arc, and tilt to the east the sediments of the Grenada Basin, bordering the volcanic arc to the west. This is not evidenced in seismic profiles acquired perpendicular to the arc, offshore the volcanic Martinique Island that has a similar size to Basse-Terre (Le Friant et al., 2015, 2003). The size of Basse-Terre Island (22 km width, culminating at only 1467 masl at La Soufrière) and its volume are also much smaller than the volume of shield volcanoes that generate such flexure.

Moreover, construction and destruction rates of the most recent volcanic edifices of Basse-Terre ( $\leq 1$  Ma) have been estimated on the basis of new radiometric ages and geomorphological modeling of the topography (Lahitte et al., 2012; Ricci et al., 2015). Height increase rates of the island has been estimated at 1 m/k.y. for the last 100 k.y. and compare with erosion rates of the volcanic edifices estimated, both chemically and mechanically that range between 0.2 and 1 m/k.y. (Rad et al., 2013; Ricci et al., 2015; Samper et al., 2007). Therefore, erosion rates compete significantly with height increase rates of the volcanoes, implying that volcano-isostatic effect promoted by the weight of the volcanoes do not contribute much in the long-term subsidence of the volcanic arc. Erosion rates in Les Saintes is probably of same order of magnitude as in Basse-Terre, and the load of the crust by the volcanic edifices is now being released by erosion, and certainly do not contribute to the subsidence rate evidenced in this study.

Finally, changes of hydro-static pressure in deep magma chambers can drive vertical deformation at the surface. By considering an elastic crust, the change in hydro-static pressure (depression) at a depth (D) can generate deformation (subsidence) up to a distance of 3D (Mogi, 1958; Gudmundsson and Nilsen 2006). The amplitude of the surface vertical deformation decreases radially and

with the increase of the depth of the reservoir, and is a function of the magma chamber radius, the pressure changes, as well as of the crust elasticity (Lamé coefficient). In the Lesser Antilles, a recent study shows that volcanic systems are fed by several interconnected small magma lenses located between a few km and the Moho depth (mush architecture, Balcone-Boissard et al., 2018). If a hydro-static pressure change occurs at the Moho depth, deformations could occur up to 90 km distance from the chamber. Several active volcanoes are located within this distance from Les Saintes plateau: the Grande Découverte-Soufrière complex in Basse-Terre is 20 km from the plateau, Morne aux Diabes and Morne Diablotins volcanic centers are located in Dominica at 30 and 45 km from Les Saintes, respectively. The emptying of their magmatic systems could contribute to the deformation (and subsidence) of the archipelago since 125 ka, assuming these deformations accumulate over long-time scales.

### **Active Faulting**

Les Saintes plateau is crosscut by a regional fault system composed of normal faults (Feuillet et al., 2002, 2010, 2011b). Some small faults crosscut the eastern part of the plateau (Fig. 2) and disrupt only locally the topography, unable to promote subsidence at the scale of the plateau.

The main normal fault of the system, the Roseau fault, extends west of the plateau. Slip on this fault produces subsidence of its hanging wall, on which lies the plateau. Slip rate along the Roseau fault is not well constrained. Its normal slip rate was estimated to be probably a few tenths of a mm/yr (Leclerc et al., 2016). Normal faults' footwall uplift to hanging-wall downdrop ratios ( $u/d$ ) have been estimated to be of 1:2 to 1:3.5 (Stein et al., 1988; Armijo et al., 1996; Ford et al., 2012) inducing a subsidence rate of the footwall equivalent to 65 to 80% of the slip rate. However, subsidence is active only in the area of fault-induced elastic flexure. Leclerc et al. (2016) proposed that the elastic flexure of Roseau fault extends only ~12 km on either side of the fault trace. This indicates that only the western half of the plateau would be influenced by the surface displacement produced by the Roseau fault. Consequently, we think that active faulting probably contributes to the subsidence of the Saintes plateau, but might not drive entirely the subsidence we estimated earlier.

### **Influence of Long-Term Subduction Processes**

In front of Guadeloupe, the prominent, isostatically uncompensated Tiburon Rise is subducting obliquely to the trench (Bouysson and Westercamp, 1990; Figs. 1 and 11). It is 1.8 km high and 30–40 km wide. This ridge is parallel to fracture zones and formed due to the North and South American plates' relative motion during mid-late Miocene (Pichot et al., 2012). It moves west-south-westward, its deep extent could be nowadays located below La Désirade and near the eastern coast of Marie-Galante Island (Fig. 11, although not imaged that deep by Evain et al., 2013).

As they subduct, bathymetric highs modify and deform accretionary prisms (e.g., Lallemand et al., 1992; Dominguez et al., 1998). They create features in the prism that can betray their path, as re-entrants, arcuate faults and troughs. Their positive topography, sometimes enhanced by their buoyancy if formed by magmatism (which is not the case for the Tiburon Rise), also promotes uplift in the prism (e.g., Hampel et al., 2004; Gerya et al., 2009, Zeumann and Hampel, 2015), a deformation evidenced in the accretionary prism offshore Guadeloupe (e.g., Evain et al., 2013).

The bathymetric highs induce deformation in the forearc, especially uplift at the initiation of their subduction, and then they promote subsidence due to margin erosion (Vannucchi et al., 2013). When subducting obliquely, they drive transient upper-plate deformation (e.g., Macharé and Orlieb, 1992; Sak et al., 2004). They create a bulge ahead of their trace that induces a rapid uplift of the coast located ahead, and a decrease of the uplift rate as the relief passes under the coast. At one location, the uplift rate varies through time and is maximum before the ridge passes below this point. By comparison, the relief of the Tiburon Rise could have promoted the rapid uplift estimated in eastern Marie-Galante and La Désirade over the late Pleistocene, and slow or no uplift of the coast since 125 ka while it is passing below the islands.

The way a volcanic arc is deforming due to the direct effect of a subducting bathymetric high is still an open question, especially as the slab is usually very deep below the arc (more than 100 km deep below Les Saintes for instance, Fig. 11A). Recently, Martinod et al. (2016) investigated this question with a visco-elastic model, and computed the deformation within an over-riding plate induced by a 3-km-high subducting ridge, from fore-arc to back-arc domains (applied to the Andean margin, modeled with a 30-km-thick crust, comparable to the crust thickness of the Lesser Antilles, Kopp et al., 2011). While subducting, a bathymetric relief produces transient uplift in the forearc, but also along the volcanic arc. The subsidence of Les Saintes volcanic islands is therefore not promoted by such processes.

On longer time scales, the stratigraphy of the forearc island carbonate platforms (and upper plateaus, Cornée et al., 2012; Léticée et al., 2008; Münch et al., 2013, 2014) also indicates that they have experienced subsidence since the Pliocene, interrupted by several episodes of emergence. The Karukera Spur shows a similar vertical motion history (De Min et al., 2015). Münch et al. (2014) propose that the subsidence of the forearc is linked to erosion of the margin by the subducting Tiburon Rise. De Min et al. (2015) propose also that the uplift events could be related to periods of strain accumulation (for instance promoted by the development of thrusts at the base of the upper plate in the forearc), and that this vertical deformation reversal could be related to changes of friction along the plate interface, induced by the ridge, over a million year. Similar mechanism has also been proposed to explain rapid reversal of upper-plate vertical motion along other subduction zones (e.g., Solomon and Vanuatu arc, Taylor et al., 2005).

Martinod et al. (2016) modeled the topographic upper-plate response of temporal variation of the interplate friction coefficient. An increase or decrease of friction coefficient can be triggered by a change in the amount of sediment

subducted, but could also be due to the subduction of a bathymetric high. They show for instance that almost as soon as an area with increased interplate friction passes the trench, the forearc and volcanic arc subside. When this specific area passes below the over-riding plate Moho, subsidence continues in the forearc but stops and changes to slow uplift in the arc. Conversely, when an area with decreased interplate friction passes the trench, the forearc and arc slightly uplift, but once this area passes the over-riding plate Moho, uplift continues in the forearc while the volcanic arc follows a transient subsidence (which stops after 1 Ma in the experiment). This latter experiment produces vertical motion histories similar and comparable to the Guadeloupe archipelago one, from the forearc to the volcanic arc. It induces that evolution of the plate interface friction over long time scales is a good candidate to explain our observations, and this would suggest that a portion of the plate interface with a relatively low friction is or has been subducting below the over-riding plate.

The way long-term deformation, linked to deep subduction processes, is accumulating in the upper plate, either continuously or gradually, remains an open question.

### ***Link between Short-Term and Long-Term Deformation***

Observations of coseismic deformation compared with the morphology of coastal areas along active margins have led many authors (e.g., Taylor et al., 1980) to consider the possibility that megathrust seismic activity generates deformation that is able to accumulate in the upper plate in the long-term. The mechanism by which short-term deformation may accumulate in the upper plate is still being investigated (e.g., Thirumalai et al., 2015) and not fully understood. Two main ideas are proposed. On one hand, long-term deformation is thought to build during megathrust earthquakes, by partial accumulation of coseismic deformation above the locked part of the interface, where the two crusts are in contact (e.g., Taylor et al., 1987, in the Vanuatu forearc and Wesson et al., 2015, and Baker et al., 2013, in the Chilean forearc), or deeper, along the segment that straddles the Moho (Melnick, 2016). On the other hand, long-term coastal morphology could be controlled by the mechanical properties of the megathrust (creeping vs stick-slip behavior) and long-term deformation consists of the accumulation of interseismic strain that is partially preserved in the upper plate (e.g., Saillard et al., 2017, along the Andean margin; van Dinther et al., 2013 in seismo-thermo-mechanical modeling).

In the Lesser Antilles, two earthquakes probably ruptured the plate interface during the historical period, in front of Martinique (11 January 1839) and between Guadeloupe and Antigua on 8 February 1843 (Fig. 1; see Feuillet et al., 2011a, for a review of the Lesser Antilles seismic activity). The 1843 earthquake generated coseismic vertical deformation in the Guadeloupe archipelago. Sainte-Claire Deville (1843) observed and reported the uplift of the eastern coast of Grande-Terre by a few tens of centimeters, and the subsidence of Pointe-à-Pitre harbor by 30 cm, along the western coast of the same island (Fig. 11). Here, this coseismic deformation pattern looks like the upper Pleistocene deformation

pattern of the Guadeloupe archipelago, where eastern coasts of the forearc islands are uplifted whereas land closer to the volcanic arc are subsiding.

Paleogeodetic studies do also provide some information about the vertical deformation produced by earthquakes breaking the plate interface. Relative sea-level reconstruction calculated from coral micro-atolls showed that the 1946 Martinique earthquake (Fig. 1), that occurred along the plate interface at depth (at the contact between the Atlantic slab and the Caribbean mantle wedge) produced coseismic subsidence of the Robert Bay (Weil-Accardo et al., 2016), consequently subsidence along the volcanic arc. It compares with the upper Pleistocene subsidence of Martinique Island, at least over the last 125 ka (Leclerc et al., 2015). Therefore, in the Lesser Antilles, the upper Pleistocene vertical deformation could accumulate through coseismic (partially uncompensated?) displacements.

To explain this coseismic deformation, Weil-Accardo et al. (2016) produced an elastic dislocation model and propose that it ruptured the plate interface between 40 and 60 km depth, where the Caribbean down-going plate is in contact with the Caribbean mantle-wedge. Recent geophysical studies tend to show that the seismogenic zone of the interface could indeed extend much deeper than what is traditionally accepted (Caribbean Moho's depth, at ~27 km in Guadeloupe, Kopp et al., 2011): on the basis of the deep seismicity, Laigle et al. (2013) propose that the down-dip limit of the seismogenic zone could reach 40–45 km, and explain such a depth by the origin and nature of the Caribbean mantle. In their recent study, based on active and passive seismic source data, Paulatto et al. (2017) image the megathrust and relate the different seismic velocities pattern to oceanic crust dehydration mechanisms. They also propose that the downdip extent of the seismogenic zone is at a depth of ~50 km, between La Désirade and Grande-Terre islands, east of Marie-Galante. If the long-term deformation mimics the coseismic one in the Lesser Antilles, then the vertical upper Pleistocene deformation pattern supports a down-dip limit of the seismogenic zone deeper than previously thought, as proposed by Laigle et al. (2013), Weil-Accardo et al. (2016), and Paulatto et al. (2017).

## **CONCLUSION**

In this study, shallow water reefs were used as markers of the interactions between tectonic movements and sea level variability over the Quaternary. We combined morphological and stratigraphic studies based on marine geophysical data with extensive reef growth modeling in order to gain knowledge about the vertical motion history along a volcanic arc.

We show that the morphology and stratigraphy of the 20-km-wide submerged Les Saintes reef plateau, lying at ~45 mbsl, presenting an unusual double barrier, and composed of several units separated by surfaces of erosion, can only be modeled in a context of subsidence. We carried out sensitivity tests on the reef growth model, in order to explore reasonable values for different parameters and different initial conditions: start time, sea level variations, basement morphology, reef growth rate, subaerial erosion rate,

and subsidence rate. With minimum constraints, our models show that Les Saintes plateau formed in a context of subsidence, and that the subsidence rate is of  $-0.3$  to  $-0.45$  m/k.y. since at least 125 ka. We even reproduced the double reef barrier, for conditions of reef growth rates  $>4.5$  m/k.y. We also modeled the plateau with subsidence rate that varies through time (modeled here since 330 ka). Appropriate synthetic cores were modeled best in cases of increasing subsidence rates with time.

By reviewing the position of MIS5e, and vertical history of the forearc islands, we confirm that regionally MIS5e deposits are deepening to the west in the Guadeloupe archipelago. We show that the subsidence in Les Saintes, along the volcanic arc, is one order of magnitude more rapid than the forearc vertical deformation rates, and not solely linked to a westward tilt of the archipelago, or to local faulting.

Deep subduction processes can drive subsidence along volcanic arc, a deformation that should be looked for along other island arcs. During subduction and over long time scales, variations in friction coefficient of the plate interface can promote transient vertical motion along both the forearc and volcanic arc that are comparable to the ones we observe (Martinod et al., 2016). Coseismic deformation not (fully) compensated over the seismic cycle is one mechanism by which the deformation could accumulate in the upper plate over long time scales. Finally, volcanic activity in the surrounding islands of Basse-Terre and Dominica could contribute to the subsidence in Les Saintes, if the deformation promoted by hydro-static changes in magmatic reservoirs can accumulate through time.

By combining marine geophysical data and reef growth modeling we showed that we can gain knowledge about upper-plate subsidence along subduction zones. Such methodology could be applied in similar tropical environments, in order to complete the picture of upper-plate vertical deformation and understand better their link to subduction parameters and processes.

#### ACKNOWLEDGMENTS

We would like to dedicate this work to our late colleague and friend Guy Cabioch with who we initiated this work. This work was funded by the French National Agency for research project ANR-05-CATT-0015 SUBSISMANTI, and research project ANR-17-CE31-0020 SERSURF. We are grateful to M. Toomey, T. Perron, and A. Ashton for constructive discussions on the different reef growth models performed in this paper, and advice regarding the manuscript, as well as J. Webster for constructive remarks on a previous version of this work. In particular, we thank M. Toomey for suggesting and designing the 1-D models testing vertical motion variations through time. We are grateful to reviewers for constructive remarks that helped improve the manuscript. This is an Institut de Physique du Globe de Paris contribution n°4002.

#### APPENDIX

To test the hypothesis that the load of Basse-Terre volcanoes, Guadeloupe, French West Indies, generates a flexure of the lithosphere and hence a deflection that affects the forearc, we assume in the following that the deformation pattern described above is taking place along a linear island arc built on an elastic plate. We apply the equations of flexure of an elastic plate developed in Fowler (2004) for a non-intact plate (as it is crosscut by faults), in order to estimate the elastic thickness  $h$  of the plate.

The elastic thickness  $h$  influences the flexural rigidity  $D$  of the plate that controls the (half-) width of the deflection ( $x_0$ ). Knowing  $x_0$  allows calculating the  $h$ , using these equations:

$$D = \frac{Eh^3}{12(1-\sigma^2)} \quad (1)$$

$$x_0 = \frac{\pi}{2} \left( \frac{4D}{(\rho_m - \rho_w)g} \right)^{\frac{1}{3}} \quad (2)$$

with  $E$  the Young's modulus,  $\sigma$  the Poisson's ratio,  $\rho_m$  and  $\rho_w$ , the mantle and water density, respectively. This calculation does not require to know either the volume of the island nor the forces applied by the load on the plate.

We define the half-width of the deflection created by the volcanic load as the distance between the topographic axis of Basse-Terre and a place where deformation is not accumulated. If we consider young deformation markers, due to uncertainties about the MIS5e sea level, we place this limit between the eastern coast of Grande-Terre, where the MIS5e is found at 5–6 masl, and the western coast of La Désirade, where it stands at 10 masl. At first order, the depression half-width ranges between 40 and 65 km. By considering a Poisson's ratio of 0.25 ( $\lambda = \mu$ ) (as in Feuillet et al., 2004), and a Young modulus of 80 GPa, we calculated that if the westward deepening was due to volcanic load induced elastic flexure, the elastic thickness of the plate would be 7–13 km.

#### REFERENCES CITED

- Adey, W.H., and Burke, R., 1976, Holocene bioherms (algal ridges and bank-barrier reefs) of the eastern Caribbean: Geological Society of America Bulletin, v. 87, no. 1, p. 95–109, [https://doi.org/10.1130/0016-7606\(1976\)87<95:HBARAB>2.0.CO;2](https://doi.org/10.1130/0016-7606(1976)87<95:HBARAB>2.0.CO;2).
- Adey, W.H., Adey, P.J., Burke, R., and Kaufman, L., 1977, The Holocene reef systems of eastern Martinique, French West Indies: Atoll Research Bulletin, Smithsonian Institution, no. 218, p. 1–40.
- Andréfouët, S., Cabioch, G., Flamand, B., and Pelletier, B., 2009, A reappraisal of the diversity of geomorphological and genetic processes of New Caledonian coral reefs: A synthesis from optical remote sensing, coring and acoustic multibeam observations: Coral Reefs, v. 28, no. 3, p. 691–707, <https://doi.org/10.1007/s00338-009-0503-y>.
- Andreieff, P., Bouysse, P., and Westercamp, D., 1989, Géologie de l'arc insulaire des Petites Antilles et évolution géodynamique de l'Est-Caraïbe: Documents du Bureau de Recherches Géologiques et Minières 171, p. 1–385.
- Anselmetti, F.S., and Eberli, G.P., 1993, Controls on sonic velocity in carbonates: Pure and Applied Geophysics, v. 141, no. 2–4, p. 287–323.
- Anselmetti, F.S., and Eberli, G.P., 2001, Sonic velocity in carbonates: A combined product of depositional lithology and diagenetic alterations, in Ginsburg, R.N., ed., Subsurface Geology of a Prograding Carbonate Platform Margin, Great Bahama Bank: Results of the Bahamas Drilling Project, SEPM (Society for Sedimentary Geology) Special Publication, v. 70, p. 193–216.
- Armijo, R., Meyer, B.G.C.P., King, G.C.P., Rigo, A., and Papanastassiou, D., 1996, Quaternary evolution of the Corinth Rift and its implications for the Late Cenozoic evolution of the Aegean: Geophysical Journal International, v. 126, no. 1, p. 11–53, <https://doi.org/10.1111/j.1365-246X.1996.tb05264.x>.
- Baker, A., Allmendinger, R.W., Owen, L.A., and Rech, J.A., 2013, Permanent deformation caused by subduction earthquakes in northern Chile: Nature Geoscience, v. 6, no. 6, p. 492–496, <https://doi.org/10.1038/ngeo1789>.
- Balcone-Boissard, H., Boudon, G., Blundy, J.D., Martel, C., Brooker, R.A., Deloule, E., Solaro, C., and Matjuschkin, V., 2018, Deep pre-eruptive storage of silicic magmas feeding Plinian and dome-forming eruptions of central and northern Dominica (Lesser Antilles) inferred from volatile contents of melt inclusions: Contributions to Mineralogy and Petrology, v. 173, <https://doi.org/10.1007/s00410-018-1528-4>.
- Barrett, S.J., and Webster, J.M., 2017, Reef Sedimentary Accretion Model (ReefSAM): Understanding coral reef evolution on Holocene time scales using 3D stratigraphic forward modelling: Marine Geology, v. 391, p. 108–126, <https://doi.org/10.1016/j.margeo.2017.07.007>.
- Battistini, R., Hirschberger, F., Hoang, C.T., and Petit, M., 1986, La basse Terrasse corallienne (Éémien) de la Guadeloupe: Morphologie, datation  $^{230}\text{Th}/^{234}\text{U}$ , néotectonique: Revue de Géomorphologie Dynamique, v. 35, p. 1–10.
- Béjar-Pizarro, M., Socquet, A., Armijo, R., Carrizo, D., Genrich, J., and Simons, M., 2013, Andean structural control on interseismic coupling in the North Chile subduction zone: Nature Geoscience, v. 6, p. 462–467, <https://doi.org/10.1038/ngeo1802>.

- Bosscher, H., and Schlager, W., 1992, Computer simulation of reef growth: *Sedimentology*, v. 39, no. 3, p. 503–512, <https://doi.org/10.1111/j.1365-3091.1992.tb02130.x>.
- Bouysse, P., and Westercamp, D., 1990, Subduction of Atlantic aseismic ridges and Late Cenozoic evolution of the Lesser Antilles island arc: *Tectonophysics*, v. 175, no. 4, p. 349–380, [https://doi.org/10.1016/0040-1951\(90\)90180-G](https://doi.org/10.1016/0040-1951(90)90180-G).
- Bouysse, P., Garrabé, F., Mauboussin, T., Andrieuff, P., Battistini, R., Carlier, P., Hinschberger, F., and Rodet, J., 1993, Carte géologique département de la Guadeloupe: Marie-Galante et îlets de la Petite-Terre, Paris, France, Bureau de Recherches Géologiques et Minières, scale 1:50,000.
- Bowin, C., 1976, Caribbean Gravity Field and Plate Tectonics: *Geological Society of America Special Paper* 169, 79 p., <https://doi.org/10.1130/SPE169>.
- Cabioch, G., 2003, Postglacial reef development in the South-West Pacific: Case studies from New Caledonia and Vanuatu: *Sedimentary Geology*, v. 159, no. 1, p. 43–59, [https://doi.org/10.1016/S0037-0738\(03\)00094-0](https://doi.org/10.1016/S0037-0738(03)00094-0).
- Camoin, G.F., Iryu Y., McInroy D.B., and the IODP Expedition 310 Scientists, 2007, IODP Expedition 310 reconstructs sea level, climatic, and environmental changes in the South Pacific during the last deglaciation: *Scientific Drilling*, v. 5, p. 4–12, <https://doi.org/10.2204/iodp.sd.5.01.2007>.
- Chlieh, M., De Chabalière, J.B., Ruegg, J.C., Armijo, R., Dmowska, R., Campos, J., and Feigl, K.L., 2004, Crustal deformation and fault slip during the seismic cycle in the North Chile subduction zone, from GPS and InSAR observations: *Geophysical Journal International*, v. 158, no. 2, p. 695–711, <https://doi.org/10.1111/j.1365-246X.2004.02326.x>.
- Cornée, J.J., Léticée, J.-L., Muench, P., Quillevère, F., Lebrun, J.-F., Moissette, P., Braga, J.-C., Melinte-Dobrinescu, M., De Min, L., Oudet, J., and Randrianasolo, A., 2012, Sedimentology, palaeoenvironments and biostratigraphy of the Pliocene–Pleistocene carbonate platform of Grande-Terre (Guadeloupe, Lesser Antilles forearc): *Sedimentology*, v. 59, no. 5, p. 1426–1451, <https://doi.org/10.1111/j.1365-3091.2011.01311.x>.
- Coudray, J., 1976, Recherches sur le Néogène et le Quaternaire marin de la Nouvelle-Calédonie: Contribution de l'étude sédimentologique à la connaissance de l'histoire géologique post-Éocène (Doctorate thesis): Fondation Singer-Polignac, v. 8, 272 p.
- Cutler, K.B., Edwards, R.L., Taylor, F.W., Cheng, H., Adkins, J., Cutler, P.M., Burr, G.S., and Bloom, A.L., 2003, Rapid sea-level fall and deep-ocean temperature change since the last interglacial period: *Earth and Planetary Science Letters*, v. 206, no. 3–4, p. 253–271, [https://doi.org/10.1016/S0012-821X\(02\)01107-X](https://doi.org/10.1016/S0012-821X(02)01107-X).
- De Min, L., Lebrun, J.-F., Cornée, J.-J., Münch, P., Léticée, J.L., Quillevère, F., Melinte-Dobrinescu, M., Randrianasolo, A., Marcaillou, B., and Zami, F., 2015, Tectonic and sedimentary architecture of the Karukéra spur: A record of the Lesser Antilles fore-arc deformations since the Neogene: *Marine Geology*, v. 363, p. 15–37, <https://doi.org/10.1016/j.margeo.2015.02.007>.
- DeMets, C., Jansma, P.E., Mattioli, G.S., Dixon, T.H., Farina, F., Bilham, R., Calais, E., and Mann, P., 2000, GPS geodetic constraints on Caribbean-North America plate motion: *Geophysical Research Letters*, v. 27, no. 3, p. 437–440, <https://doi.org/10.1029/1999GL005436>.
- Deplus, C., and Feuillet, N., 2010, BATHYSAINTES cruise, RV *Pourquoi Pas?*, <https://doi.org/10.17600/10030020>.
- Dominguez, S., Lallemand, S.E., Malavieille, J., and von Huene, R., 1998, Upper plate deformation associated with seamount subduction: *Tectonophysics*, v. 293, no. 3–4, p. 207–224, [https://doi.org/10.1016/S0040-1951\(98\)00086-9](https://doi.org/10.1016/S0040-1951(98)00086-9).
- Dullo, W.-C., 2005, Coral growth and reef growth: A brief review: *Facies*, v. 51, no. 1–4, p. 33–48, <https://doi.org/10.1007/s10347-005-0060-y>.
- Dutton, A., and Lambeck, K., 2012, Ice volume and sea level during the last interglacial: *Science*, v. 337, p. 216–219.
- Evain, M., Galve, A., Charvis, P., Laigle, M., Kopp, H., Bécél, A., Weinzierl, W., Hirn, A.I., Flueh, E.R., and Gallart, J., 2013, Structure of the Lesser Antilles subduction forearc and backstop from 3D seismic refraction tomography: *Tectonophysics*, v. 603, p. 55–67, <https://doi.org/10.1016/j.tecto.2011.09.021>.
- Feuillet, N., Manighetti, I., and Tapponnier, P., 2002, Arc parallel extension and localization of volcanic complexes in Guadeloupe, Lesser Antilles: *Journal of Geophysical Research*. *Solid Earth*, v. 107, no. B12, <https://doi.org/10.1029/2001JB000308>.
- Feuillet, N., Tapponnier, P., Manighetti, I., Villemant, B., and King, G.C.P., 2004, Differential uplift and tilt of Pleistocene reef platforms and Quaternary slip rate on the Morne-Piton normal fault (Guadeloupe, French West Indies): *Journal of Geophysical Research*. *Solid Earth*, v. 109, <https://doi.org/10.1029/2003JB002496>.
- Feuillet, N., Leclerc, F., Tapponnier, P., Beauducel, F., Boudon, G., Le Friant, A., Deplus, C., Lebrun, J.-F., Nercessian, A., Saurel, J.-M., and Clément, V., 2010, Active faulting induced by slip partitioning in Montserrat and link with volcanic activity: New insights from the 2009 GWADASEIS marine cruise data: *Geophysical Research Letters*, v. 37, no. 19, <https://doi.org/10.1029/2010GL042556>.
- Feuillet, N., Beauducel, F., and Tapponnier, P., 2011a, Tectonic context of moderate to large historical earthquakes in the Lesser Antilles and mechanical coupling with volcanoes: *Journal of Geophysical Research*. *Solid Earth*, v. 116, no. B10, <https://doi.org/10.1029/2011JB008443>.
- Feuillet, N., Beauducel, F., Jacques, E., Tapponnier, P., Delouis, B., Bazin, S., Vallée, M., and King, G.C.P., 2011b, The Mw = 6.3, November 21, 2004, Les Saintes earthquake (Guadeloupe): Tectonic setting, slip model and static stress changes: *Journal of Geophysical Research*. *Solid Earth*, v. 116, no. B10, <https://doi.org/10.1029/2011JB008310>.
- Ford, M., Rohais, S., Williams, E.A., Bourlange, S., Jousset, D., Backert, N., and Malartre, F., 2012, Tectono-sedimentary evolution of the western Corinth rift (Central Greece): *Basin Research*, v. 25, p. 3–25.
- Fowler, C.M.R., 2004, *The Solid Earth: An Introduction to Global Geophysics* (second edition): Cambridge, UK, Cambridge University Press, 685 p., <https://doi.org/10.1017/CBO9780511819643>.
- Garrabé, F., and Paulin, C., 1984, Découverte par forage de calcaires à Polypiers Pléistocène sous le Piedmont volcano-sédimentaire du Nord-Est de la Basse-Terre de Guadeloupe: Principaux résultats scientifiques et techniques: Orléans, France, Bureau de Recherches Géologiques et Minières, 72 p.
- Gerya, T.V., Fossati, D., Cantieni, C., and Seward, D., 2009, Dynamic effects of aseismic ridge subduction: Numerical modelling: *European Journal of Mineralogy*, v. 21, no. 3, p. 649–661, <https://doi.org/10.1127/0935-1221/2009/0021-1931>.
- Gischler, E., 2008, Accretion patterns in Holocene tropical coral reefs: Do massive coral reefs in deeper water with slowly growing corals accrete faster than shallower branched coral reefs with rapidly growing corals?: *International Journal of Earth Sciences*, v. 97, no. 4, p. 851–859, <https://doi.org/10.1007/s00531-007-0201-3>.
- Grant, K.M., Rohling, E.J., Bronk Ramsey, C., Cheng, H., Edwards, R.L., Florindo, F., Heslop, D., Marra, F., Roberts, A.P., Tamisiea, M.E., and Williams, F., 2014, Sea-level variability over five glacial cycles: *Nature Communications*, v. 5, 5076, <https://doi.org/10.1038/ncomms6076>.
- Grigg, R.W., 1997, Paleogeography of coral reefs in the Hawaiian-Emperor Chain: Revisited: *Coral Reefs*, v. 16, p. S33–S38, <https://doi.org/10.1007/s003380050239>.
- Gudmundsson, A., and Nilsen, K., 2006, Ring-faults in composite volcanoes: Structures, models and stress fields associated with their formation, in Troise, C., De Natale, G., and Kilburn, C.R.J., eds., *Mechanisms of Activity and Unrest at Large Calderas*: Geological Society of London Special Publication 269, no. 1, p. 83–108, <https://doi.org/10.1144/GSL.SP2006.269.01.06>.
- Hempel, A., Kukowski, N., Bialas, J., Huebscher, C., and Heinbockel, R., 2004, Ridge subduction at an erosive margin: The collision zone of the Nazca Ridge in southern Peru: *Journal of Geophysical Research*. *Solid Earth*, v. 109, <https://doi.org/10.1029/2003JB002593>.
- Henry, H., Regard, V., Pardoja, K., Husson, L., Martinod, J., Witt, C., and Heuret, A., 2014, Upper Pleistocene uplifted shorelines as tracers of (local rather than global) subduction dynamics: *Journal of Geodynamics*, v. 78, p. 8–20, <https://doi.org/10.1016/j.jog.2014.04.001>.
- Hubbard, D.K., 2009, Depth-related and species-related patterns of Holocene reef accretion in the Caribbean and western Atlantic: A critical assessment of existing models, in Swart, P.K., Eberli, G.P., McKenzie, J.A., Jarvis, I., and Stevens, T., eds., *Perspectives in Carbonate Geology: A Tribute to the Career of Robert Nathan Ginsburg*: Hoboken, New Jersey, USA, Wiley-Blackwell, Inc., p. 1–18, <https://doi.org/10.1002/9781444312065.ch1>.
- Jacques, D., and Maury, R.C., 1988, L'archipel des Saintes (Guadeloupe, Petites Antilles): *Géologie et Pétrologie: Géologie de la France*, v. 23, p. 89–99.
- Jara-Muñoz, J., Melnick, D., Brill, D., and Strecker, M.R., 2015, Segmentation of the 2010 Maule Chile earthquake rupture from a joint analysis of uplifted marine terraces and seismic-cycle deformation patterns: *Quaternary Science Reviews*, v. 113, p. 171–192, <https://doi.org/10.1016/j.quascirev.2015.01.005>.
- Jara-Muñoz, J., Melnick, D., Zambrano, P., Rietbrock, A., González, J., Argandoña, B., and Strecker, M.R., 2017, Quantifying offshore fore-arc deformation and splay-fault slip using drowned Pleistocene shorelines, Arauco Bay, Chile: *Journal of Geophysical Research*. *Solid Earth*, v. 122, no. 6, p. 4529–4558, <https://doi.org/10.1002/2016JB013339>.
- Khan, N.S., Ashe, E., Horton, B.P., Dutton, A., Kopp, R.E., Brocard, G., Engelhart, S.E., Hill, D.F., Peltier, W.R., Vane, C.H., and Scatena, F.N., 2017, Drivers of Holocene sea-level change in the Caribbean: *Quaternary Science Reviews*, v. 155, p. 13–36, <https://doi.org/10.1016/j.quascirev.2016.08.032>.
- Koelling, M., Webster, J.M., Camoin, G., Iryu, Y., Bard, E., and Seard, C., 2009, SEALEX—Internal reef chronology and virtual drill logs from a spreadsheet-based reef growth model: *Global and Planetary Change*, v. 66, p. 149–159, <https://doi.org/10.1016/j.gloplacha.2008.07.011>.

- Kopp, H., Weinzierl, W., Becel, A., Charvis, P., Evain, M., Flueh, E.R., Gailler, A., Galve, A., Hirn, A., Kandilarov, A., Klaeschen, D., Laigle, M., Papenberg, C., Planert, L., Roux, E., and Trail and Thales teams, 2011, Deep structure of the central Lesser Antilles Island Arc: Relevance for the formation of continental crust: *Earth and Planetary Science Letters*, v. 304, no. 1, p. 121–134, <https://doi.org/10.1016/j.epsl.2011.01.024>.
- Kopp, R.E., Simons, F.J., Mitrovica, J.X., Maloof, A.C., and Oppenheimer, M., 2009, Probabilistic assessment of sea level during the last interglacial stage: *Nature*, v. 462, p. 863–867, <https://doi.org/10.1038/nature08686>.
- Lahitte, P., Samper, A., and Quidelleur, X., 2012, DEM-based reconstruction of southern Basse-Terre volcanoes (Guadeloupe archipelago, FWI): Contribution to the Lesser Antilles Arc construction rates and magma production: *Geomorphology*, v. 136, no. 1, p. 148–164, <https://doi.org/10.1016/j.geomorph.2011.04.008>.
- Laigle, M., Hirn, A., Sapin, M., Bécel, A., Charvis, P., Flueh, E., Diaz, J., Lebrun, J.-F., Gesret, A., Raffaele, R., Galvé, A., Evain, M., Ruiz, M., Kopp, H., Bayrakci, G., Weinzierl, W., Hello, Y., Lépine, J.-C., Viodé, J.-P., Sachpazi, M., Gallart, J., Kissling, E., and Nicolich, R., 2013, Seismic structure and activity of the north-central Lesser Antilles subduction zone from an integrated approach: Similarities with the Tohoku forearc: *Tectonophysics*, v. 603, p. 1–20, <https://doi.org/10.1016/j.tecto.2013.05.043>.
- Lajoie, K.R., 1986, Coastal tectonics, in Wallace, R.E., ed., *Active Tectonics*: Washington, D.C., National Academy Press, p. 95–124.
- Lallemand, S.E., Malavielle, J., and Calassou, S., 1992, Effects of oceanic ridge subduction on accretionary wedges: Experimental modeling and marine observations: *Tectonics*, v. 11, no. 6, p. 1301–1313, <https://doi.org/10.1029/92TC00637>.
- Lardeaux, J.M., Münch, P., Corsini, M., Cornée, J.J., Verati, C., Lebrun, J.F., Quillévéré, F., Melinte-Dobrinescu, M., Léticée, J.L., Fietzke, J., and Mazabraud, Y., 2013, La Désirade island (Guadeloupe, French West Indies): A key target for deciphering the role of reactivated tectonic structures in Lesser Antilles arc building: *Bulletin de la Société Géologique de France*, v. 184, no. 1–2, p. 21–34, <https://doi.org/10.2113/gssgfbull.184.1-2.21>.
- Le Friant, A., Boudon, G., Deplus, C., and Villemant, B., 2003, Large-scale flank collapse events during the activity of Montagne Pelée, Martinique, Lesser Antilles: *Journal of Geophysical Research. Solid Earth*, v. 108, <https://doi.org/10.1029/2001JB001624>.
- Le Friant, A., Ishizuka, O., Boudon, G., Palmer, M.R., Talling, P.J., Villemant, B., Adachi, T., Aljehdali, M., Breitzkreuz, C., Brunet, M., and Caron, B., 2015, Submarine record of volcanic island construction and collapse in the Lesser Antilles arc: First scientific drilling of submarine volcanic island landslides by IODP Expedition 340: *Geochemistry, Geophysics, Geosystems*, v. 16, no. 2, p. 420–442, <https://doi.org/10.1002/2014GC005652>.
- Lebrun, J.F., 2009, KASHALLOW 2 cruise, RV *Le Suroît*, <https://doi.org/10.17600/9020010>.
- Leclerc, F., Feuillet, N., Cabioch, G., Deplus, C., Lebrun, J.F., BATHYSAINTEs cruise scientific party, Bazin, S., Beauducel, F., Boudon, G., LeFriant, A., De Min, L., and Melezan, D., 2014, The Holocene drowned reef of Les Saintes plateau as witness of a long-term tectonic subsidence along the Lesser Antilles volcanic arc in Guadeloupe: *Marine Geology*, v. 355, p. 115–135, <https://doi.org/10.1016/j.margeo.2014.05.017>.
- Leclerc, F., Feuillet, N., Perret, M., Cabioch, G., Bazin, S., Lebrun, J.-F., and Saurel, J.M., 2015, The reef platform of Martinique: Interplay between eustasy, tectonic subsidence and volcanism since Late Pleistocene: *Marine Geology*, v. 369, p. 34–51, <https://doi.org/10.1016/j.margeo.2015.08.001>.
- Leclerc, F., Feuillet, N., and Deplus, C., 2016, Interactions between active faulting, volcanism and sedimentary processes at an island arc: Insights from Les Saintes channel, Lesser Antilles arc: *Geochemistry, Geophysics, Geosystems*, v. 17, p. 2781–2802, <https://doi.org/10.1002/2016GC006337>.
- Léticée, J.-L., 2008, Architecture d'une plateforme carbonatée insulaire plio-pleistocène en domaine de marge active (avant-arc des Petites Antilles, Guadeloupe): Chronostratigraphie, sédimentologie paléoenvironnements [unpublished Ph.D. thesis]: Pointe à Pitre, Université des Antilles et de la Guyane, 261 p., <http://www.diffusiontheses.fr/59450-these-de-leticee-jean-len.html>.
- Léticée, J.-L., Cornée, J.-J., Münch, P., Fietzke, J., Philippon, M., Lebrun, J.-F., De Min, L., and Randrianasolo, A., 2019, Decreasing uplift rates and Pleistocene marine terraces settlement in the central lesser Antilles fore-arc (La Désirade Island, 16° N): *Quaternary International*, v. 508, p. 43–59, <https://doi.org/10.1016/j.quaint.2018.10.030>.
- Macharé, J., and Ortlieb, L., 1992, Plio-Quaternary vertical motions and the subduction of the Nazca Ridge, central coast of Peru: *Tectonophysics*, v. 205, no. 1, p. 97–108, [https://doi.org/10.1016/0040-1951\(92\)90420-B](https://doi.org/10.1016/0040-1951(92)90420-B).
- Macintyre, I.G., 1972, Submerged reefs of eastern Caribbean: *AAPG Bulletin*, v. 56, no. 4, p. 720–738.
- Martinod, J., Regard, V., Letourmy, Y., Henry, H., Hassani, R., Baratchart, S., and Carretier, S., 2016, How do subduction processes contribute to forearc Andean uplift?: Insights from numerical models: *Journal of Geodynamics*, v. 96, p. 6–18, <https://doi.org/10.1016/j.jog.2015.04.001>.
- Melnick, D., 2016, Rise of the central Andean coast by earthquakes straddling the Moho: *Nature Geoscience*, v. 9, p. 401–407, <https://doi.org/10.1038/ngeo2683>.
- Melnick, D., Moreno, M., Motagh, M., Cisternas, M., and Wesson, R.L., 2012, Splay fault slip during the Mw 8.8 2010 Maule Chile earthquake: *Geology*, v. 40, p. 251–254, <https://doi.org/10.1130/G32712.1>.
- Mogi, K., 1958, Relations between the eruptions of various volcanoes and the deformations of the ground surfaces around them: *Bulletin of the Earthquake Research Institute*, v. 36, p. 99–134.
- Moore, J.G., 1970, Relationship between subsidence and volcanic load, Hawaii: *Bulletin Volcanologique*, v. 34, no. 2, p. 562–576, <https://doi.org/10.1007/BF02596771>.
- Münch, P., Lebrun, J.-F., Cornée, J.-J., Thionin, I., Guennoc, P., Marcaillou, B.J., Begot, J., Bertrand, G., De Berc, S.B., Biscarrat, K., Claud, C., De Min, L., Fournier, F., Gailler, L., Graindorge, D., Léticée, J.-L., Marie, L., Mazabraud, Y., Melinte-Dobrinescu, M., Moissette, P., Quillévéré, F., Verati, C., and Randrianasolo, A., 2013, Pliocene to Pleistocene carbonate systems of the Guadeloupe archipelago, French Lesser Antilles: A land and sea study (the KaShallow project): *Bulletin de la Société Géologique de France*, v. 184, no. 1–2, p. 99–110, <https://doi.org/10.2113/gssgfbull.184.1-2.99>.
- Münch, P., Cornée, J.J., Lebrun, J.F., Quillevere, F., Verati, C., Melinte-Dobrinescu, M., Demory, F., Smith, B., Jourdan, F., Lardeaux, J.M., and De Min, L., 2014, Pliocene to Pleistocene vertical movements in the forearc of the Lesser Antilles subduction: Insights from chronostratigraphy of shallow-water carbonate platforms (Guadeloupe archipelago): *Journal of the Geological Society*, v. 171, no. 3, p. 329–341, <https://doi.org/10.1144/jgs2013.005>.
- Neumann, A.C., and Macintyre, I., 1985, Reef response to sea level rise: Keep-up, catch-up or give-up: *Proceedings of the Fifth International Coral Reef Congress, Tahiti, 27 May–1 June*, v. 3, p. 105–110.
- Opdyke, N.D., Spangler, D.P., Smith, D.L., Jones, D.S., and Lindquist, R.C., 1984, Origin of the epeirogenic uplift of Pliocene-Pleistocene beach ridges in Florida and development of the Florida karst: *Geology*, v. 12, no. 4, p. 226–228, [https://doi.org/10.1130/0091-7613\(1984\)12<226:OOTEUO>2.0.CO;2](https://doi.org/10.1130/0091-7613(1984)12<226:OOTEUO>2.0.CO;2).
- Paulatto, M., Laigle, M., Galve, A., Charvis, P., Sapin, M., Bayrakci, G., Evain, M., and Kopp, H., 2017, Dehydration of subducting slow-spread oceanic lithosphere in the Lesser Antilles: *Nature Communications*, v. 8, no. 15980, <https://doi.org/10.1038/ncomms15980>.
- Pedoja, K., Husson, L., Regard, V., Cobbold, P.R., Oustanciaux, E., Johnson, M.E., Kershaw, S., Saillard, M., Martinod, J., Furgerot, L., Weill, P., and Delcaillau, B., 2011, Relative sea-level fall since the last interglacial stage: Are coasts uplifting worldwide?: *Earth-Science Reviews*, v. 108, no. 1–2, p. 1–15, <https://doi.org/10.1016/j.earscirev.2011.05.002>.
- Pedoja, K., Husson, L., Johnson, M.E., Melnick, D., Witt, C., Pochat, S., Nexer, M., Delcaillau, B., Pinégina, T., Poprawski, Y., Authemayou, C., Elliot, M., Regard, V., and Garestier, F., 2014, Coastal staircase sequences reflecting sea-level oscillations and tectonic uplift during the Quaternary and Neogene: *Earth-Science Reviews*, v. 132, p. 13–38, <https://doi.org/10.1016/j.earscirev.2014.01.007>.
- Philibosian, B., Sieh, K., Avouac, J.-P., Natawidjaja, D.H., Chiang, H.-W., Wu, C.-C., Shen, C.-C., Daryono, M.R., Perfettini, H., Suwargadi, B.W., Lu, Y., and Wang, X., 2017, Earthquake supercycles on the Mentawai segment of the Sunda megathrust in the seventeenth century and earlier: *Journal of Geophysical Research. Solid Earth*, v. 122, no. 1, p. 642–676, <https://doi.org/10.1002/2016JB013560>.
- Pichot, T., Patriat, M., Westbrook, G.K., Nalpas, T., Gutscher, M.A., Roest, W.R., Deville, E., Moulin, M., Aslanian, D., and Rabineau, M., 2012, The Cenozoic tectonostratigraphic evolution of the Barracuda Ridge and Tiburon Rise, at the western end of the North America-South America plate boundary zone: *Marine Geology*, v. 303, p. 154–171, <https://doi.org/10.1016/j.margeo.2012.02.001>.
- Rad, S., Rivé, K., Vittecoq, B., Cerdan, O., and Allègre, C.J., 2013, Chemical weathering and erosion rates in the Lesser Antilles: An overview in Guadeloupe, Martinique and Dominica: *Journal of South American Earth Sciences*, v. 45, p. 331–344, <https://doi.org/10.1016/j.jsames.2013.03.004>.
- Ricci, J., Lahitte, P., and Quidelleur, X., 2015, Construction and destruction rates of volcanoes within tropical environment: Examples from the Basse-Terre Island (Guadeloupe, Lesser Antilles): *Geomorphology*, v. 228, p. 597–607, <https://doi.org/10.1016/j.geomorph.2014.10.002>.
- Rooney, J.J., Wessel, P., Hoeke, R., Weiss, J., Baker, J., Parrish, F., Fletcher, C.H., Chojnacki, J., Garcia, M., Brainard, R., and Vroom, P., 2008, Geology and geomorphology of coral reefs in the



- northwestern Hawaiian Islands, *in* Riegl, B.M., and Dodge, R.E., eds., *Coral Reefs of the USA: Dordrecht, The Netherlands, Springer*, v. 13, p. 519–571, [https://doi.org/10.1007/978-1-4020-6847-8\\_13](https://doi.org/10.1007/978-1-4020-6847-8_13).
- Saillard, M., Hall, S.R., Audin, L., Farber, D.L., Regard, V., and Hérail, G., 2011, Andean coastal uplift and active tectonics in southern Peru:  $^{10}\text{Be}$  surface exposure dating of differentially uplifted marine terrace sequences (San Juan de Marcona, 15.4°S): *Geomorphology*, v. 128, p. 178–190, <https://doi.org/10.1016/j.geomorph.2011.01.004>.
- Saillard, M., Audin, L., Rousset, B., Avouac, J.-P., Chlieh, M., Hall, S.R., Husson, L., and Farber, D.L., 2017, From the seismic cycle to long-term deformation: linking seismic coupling and Quaternary coastal geomorphology along the Andean megathrust: *Tectonics*, v. 36, no. 2, p. 241–256, <https://doi.org/10.1002/2016TC004156>.
- Sainte-Claire Deville, C., 1843, *Observations sur le tremblement de terre éprouvé à la Guadeloupe le 8 Février 1843: Imprimerie du Gouverneur, Basse-Terre, Guadeloupe*.
- Sak, P.B., Fisher, D.M., and Gardner, T.W., 2004, Effects of subducting seafloor roughness on upper plate vertical tectonism: Osa Peninsula, Costa Rica: *Tectonics*, v. 23, no. 1, <https://doi.org/10.1029/2002TC001474>.
- Samper, A., Quidelleur, X., Lahitte, P., and Mollex, D., 2007, Timing of effusive volcanism and collapse events within an oceanic arc island: Basse-Terre, Guadeloupe archipelago (Lesser Antilles Arc): *Earth and Planetary Science Letters*, v. 258, no. 1–2, p. 175–191, <https://doi.org/10.1016/j.epsl.2007.03.030>.
- Savage, J.C., 1983, A dislocation model of strain accumulation and release at a subduction zone: *Journal of Geophysical Research. Solid Earth*, v. 88, no. B6, p. 4984–4996.
- Schellmann, G., and Radtke, U., 2004, A revised morpho- and chronostratigraphy of the late and middle Pleistocene coral reef terraces on Southern Barbados (West Indies): *Earth-Science Reviews*, v. 64, p. 157–187, [https://doi.org/10.1016/S0012-8252\(03\)00043-6](https://doi.org/10.1016/S0012-8252(03)00043-6).
- Shakun, J.D., Lea, D.W., Lisiecki, L., and Raymo, M.E., 2015, An 800-kyr record of global surface ocean  $\delta^{18}\text{O}$  and implications for ice volume-temperature coupling: *Earth and Planetary Science Letters*, v. 426, p. 58–68, <https://doi.org/10.1016/j.epsl.2015.05.042>.
- Siddall, M., Chappell, J., and Potter, E.K., 2007, Eustatic sea level during past interglacials, *in* Sirocco, F., Claussen, M., Sánchez Goñi, M.F., and Litt, T., eds., *The Climate of Past Interglacials: Developments in Quaternary Sciences*, v. 7: Elsevier, p. 75–92, [https://doi.org/10.1016/S1571-0866\(07\)80032-7](https://doi.org/10.1016/S1571-0866(07)80032-7).
- Sieh, K., Natawidjaja, D.H., Meltzner, A.J., Shen, C.C., Cheng, H., Li, K.S., Suwargadi, B.W., Galetzka, J., Philibosian, B., and Edwards, R.L., 2008, Earthquake supercycles inferred from sea-level changes recorded in the corals of West Sumatra: *Science*, v. 322, p. 1674–1678, <https://doi.org/10.1126/science.1163589>.
- Spencer, T., 1985, Weathering rates on a Caribbean reef limestone: Results and implications: *Marine Geology*, v. 69, no. 1–2, p. 195–201, [https://doi.org/10.1016/0025-3227\(85\)90142-2](https://doi.org/10.1016/0025-3227(85)90142-2).
- Stein, R.S., King, G.C.P., and Rundle, J.B., 1988, The growth of geological structures by repeated earthquakes 2. Field examples of continental dip-slip faults: *Journal of Geophysical Research. Solid Earth*, v. 93, no. B11, p. 13319–13331, <https://doi.org/10.1029/JB093iB11p13319>.
- Tallarico, A., Dragoni, M., Anzidei, M., and Esposito, A., 2003, Modeling long-term ground deformation due to the cooling of a magma chamber: Case of Basiluzzo island, Aeolian Islands, Italy: *Journal of Geophysical Research. Solid Earth*, v. 108, no. B12, <https://doi.org/10.1029/2002JB002376>.
- Taylor, F.W., Isacks, B.L., Jouannic, C., Bloom, A.L., and Dubois, J., 1980, Coseismic and Quaternary vertical tectonic movements, Santo and Malekula Islands, New Hebrides Island Arc: *Journal of Geophysical Research. Solid Earth*, v. 85, no. B10, p. 5367–5381, <https://doi.org/10.1029/JB085iB10p05367>.
- Taylor, F.W., Frohlich, C., Lecolle, J., and Strecker, M., 1987, Analysis of partially emerged corals and reef terraces in the central Vanuatu arc: Comparison of contemporary coseismic and nonseismic with Quaternary vertical movements: *Journal of Geophysical Research. Solid Earth*, v. 92, no. B6, p. 4905–4933, <https://doi.org/10.1029/JB092iB06p04905>.
- Taylor, F.W., Mann, P., Bevis, M.G., Edwards, R.L., Cheng, H., Cutler, K.B., Gray, S.C., Burr, G.S., Beck, J.W., Phillips, D.A., and Recy, J., 2005, Rapid forearc uplift and subsidence caused by impinging bathymetric features: Examples from the New Hebrides and Solomon arcs: *Tectonics*, v. 24, no. 6, <https://doi.org/10.1029/2004TC001650>.
- Thirumalai, K., Taylor, F.W., Shen, C.-C., Lavier, L.L., Frohlich, C., Wallace, L., Wu, C.-C., Sun, H., and Papabatu, A.K., 2015, Variable Holocene deformation above a shallow subduction zone extremely close to the trench: *Nature Communications*, v. 6, 7607, <https://doi.org/10.1038/ncomms8607>.
- Toomey, M., Ashton, A.D., and Perron, J.T., 2013, Profiles of ocean island coral reefs controlled by sea-level history and carbonate accumulation rates: *Geology*, v. 41, p. 731–734, <https://doi.org/10.1130/G34109.1>.
- van Dinther, Y., Gerya, T.V., Dalguer, L.A., Mai, P.M., Morra, G., and Giardini, D., 2013, The seismic cycle at subduction thrusts: Insights from seismo-thermomechanical models: *Journal of Geophysical Research. Solid Earth*, v. 118, no. 12, p. 6183–6202, <https://doi.org/10.1002/2013JB010380>.
- Vannucchi, P., Sak, P.B., Morgan, J.P., Ohkushi, K., Ujiie, K., and the IODP Expedition 334 Shipboard Scientists, 2013, Rapid pulses of uplift, subsidence, and subduction erosion offshore Central America: Implications for building the rock record of convergent margins: *Geology*, v. 41, no. 9, p. 995–998, <https://doi.org/10.1130/G34355.1>.
- Vérati, C., Mazabraud, Y., Lardeaux, J.-M., Corsini, M., Schneider, D., Voitov, E., and Zami, F., 2016, Tectonic evolution of Les Saintes archipelago (Guadeloupe, French West Indies): Relation with the Lesser Antilles arc system: *Bulletin de la Société Géologique de France*, v. 187, no. 1, p. 3–10, <https://doi.org/10.2113/gssgfbull.187.1.3>.
- Villemant, B., and Feuillet, N., 2003, Dating open systems by the  $^{238}\text{U}$ - $^{234}\text{U}$ - $^{230}\text{Th}$  method: Application to Quaternary reef terraces: *Earth and Planetary Science Letters*, v. 210, no. 1–2, p. 105–118, [https://doi.org/10.1016/S0012-821X\(03\)00100-6](https://doi.org/10.1016/S0012-821X(03)00100-6).
- Waelbroeck, C., Labeyrie, L., Michel, E., Duplessy, J.C., McManus, J.F., Lambeck, K., Balbon, E., and Labracherie, M., 2002, Sea-level and deep water temperature changes derived from benthic foraminifera isotopic records: *Quaternary Science Reviews*, v. 21, no. 1, p. 295–305, [https://doi.org/10.1016/S0277-3791\(01\)00101-9](https://doi.org/10.1016/S0277-3791(01)00101-9).
- Walcott, R.I., 1970, Flexure of the lithosphere at Hawaii: *Tectonophysics*, v. 9, no. 5, p. 435–446, [https://doi.org/10.1016/0040-1951\(70\)90056-9](https://doi.org/10.1016/0040-1951(70)90056-9).
- Wang, Y., Shyu, J.B.H., Sieh, K., Chiang, H.W., Wang, C.C., Aung, T., Lin, Y.N.N., Shen, C.C., Min, S., Than, O., and Lin, K.K., 2013, Permanent upper plate deformation in western Myanmar during the great 1762 earthquake: Implications for neotectonic behavior of the northern Sunda megathrust: *Journal of Geophysical Research. Solid Earth*, v. 118, no. 3, p. 1277–1303, <https://doi.org/10.1002/jgrb.50121>.
- Weil-Accardo, J., 2014, *Paléoisosmicité, cycle sismique et couplage tectonique de la subduction antillaise par l'étude des microatolls coralliens et des terrasses marines [Ph.D. dissertation]: Paris, France, Paris Diderot University, Institut de Physique du Globe de Paris*.
- Weil-Accardo, J., Feuillet, N., Jacques, E., Deschamps, P., Beauducel, F., Cabioch, G., Tapponnier, P., Saurel, J.-M., and Galetzka, J., 2016, Two hundred thirty years of relative sea level changes due to climate and megathrust tectonics recorded in coral microatolls of Martinique (French West Indies): *Journal of Geophysical Research. Solid Earth*, v. 121, no. 4, p. 2873–2903, <https://doi.org/10.1002/2015JB012406>.
- Wesson, R.L., Melnick, D., Cisternas, M., Moreno, M., and Ely, L.L., 2015, Vertical deformation through a complete seismic cycle at Isla Santa Maria, Chile: *Nature Geoscience*, v. 8, p. 547–551, <https://doi.org/10.1038/ngeo2468>.
- Zachariasen, J., Sieh, K., Taylor, F.W., and Hantoro, W.S., 2000, Modern vertical deformation above the Sumatran subduction zone: Paleogeodetic insights from coral microatolls: *Bulletin of the Seismological Society of America*, v. 90, p. 897–913, <https://doi.org/10.1785/0119980016>.
- Zami, F., Quidelleur, X., Ricci, J., Lebrun, J.F., and Samper, A., 2014, Initial sub-aerial volcanic activity along the central Lesser Antilles inner arc: New K-Ar ages from Les Saintes volcanoes: *Journal of Volcanology and Geothermal Research*, v. 287, p. 12–21, <https://doi.org/10.1016/j.jvolgeores.2014.09.011>.
- Zeumann, S., and Hampel, A., 2015, Deformation of erosive and accretive forearcs during subduction of migrating and non-migrating aseismic ridges: Results from 3-D finite element models and application to the Central American, Peruvian, and Ryukyu margins: *Tectonics*, v. 34, no. 9, p. 1769–1791, <https://doi.org/10.1002/2015TC003867>.
- Zinke, J., Reijmer, J.J.G., and Thomassin, B.A., 2001, Seismic architecture and sediment distribution within the Holocene barrier reef-lagoon complex of Mayotte (Comoro archipelago, SW Indian Ocean): *Palaeogeography, Palaeoclimatology, Palaeoecology*, v. 175, no. 1, p. 343–368, [https://doi.org/10.1016/S0031-0182\(01\)00379-0](https://doi.org/10.1016/S0031-0182(01)00379-0).